SEDIMENTOLOGY the journal of the International Association of Sedimentologists

Sedimentology (2016) **63**, 1474–1506 doi: 10.1111/sed.12270

Facies model for a coarse-grained, tide-influenced delta: Gule Horn Formation (Early Jurassic), Jameson Land, Greenland

CHRISTIAN HAUG EIDE*†, JOHN A. HOWELL*[1], SIMON J. BUCKLEY*, ALLARD W. MARTINIUS‡, BJØRN TERJE OFTEDAL‡ and GIJS A. HENSTRA†
**Uni Research CIPR, P.O. Box 7810, N-5020 Bergen, Norway (E-mail: christian.eide@uib.no)*
†Department of Earth Science, University of Bergen, P.O. Box 7803, N-5020 Bergen, Norway
‡Statoil ASA, 7500 Stjørdal, Norway

Associate Editor – Mariano Marzo

ABSTRACT

Tide-dominated deltas have an inherently complex distribution of heterogeneities on several different scales and are less well-understood than their wave-dominated and river-dominated counterparts. Depositional models of these environments are based on a small set of ancient examples and are, therefore, immature. The Early Jurassic Gule Horn Formation is particularly well-exposed in extensive sea cliffs from which a 32 km long, 250 m high virtual outcrop model has been acquired using helicopter-mounted light detection and ranging (LiDAR). This dataset, combined with a set of sedimentological logs, facilitates interpretation and measurement of depositional elements and tracing of stratigraphic surfaces over seismic-scale distances. The aim of this article is to use this dataset to increase the understanding of depositional elements and lithologies in proximal, unconfined, tide-dominated deltas from the delta plain to prodelta. Deposition occurred in a structurally controlled embayment, and immature sediments indicate proximity to the sediment source. The succession is tide dominated but contains evidence for strong fluvial influence and minor wave influence. Wave influence is more pronounced in transgressive intervals. Nine architectural elements have been identified, and their internal architecture and stratigraphical distribution has been investigated. The distal parts comprise prodelta, delta front and unconfined tidal bar deposits. The medial part is characterized by relatively narrow, amalgamated channel fills with fluid mud-rich bases and sandier deposits upward, interpreted as distributary channels filled by tidal bars deposited near the turbidity maximum. The proximal parts of the studied system are dominated by sandy distributary channel and heterolithic tidal-flat deposits. The sandbodies of the proximal tidal channels are several kilometres wide and wider than exposures in all cases. Parasequence boundaries are easily defined in the prodelta to delta-front environments, but are difficult to trace into the more proximal deposits. This article illustrates the proximal to distal organization of facies in unconfined tide-dominated deltas and shows how such environments react to relative sea-level rise.

Keywords Delta, deltaic, Elis Bjerg, facies model, tidal bar, tidal delta, tide dominated, Tilje Formation.

[1]Present address: Department of Geology & Petroleum Geology, Meston Building, University of Aberdeen, Aberdeen AB24 3UE, UK.

INTRODUCTION

Tidal depositional systems are characterized by cyclical and rapid variations in flow velocity and, therefore, have inherently complex heterogeneities and incision on several different scales (e.g. Willis, 2005; Dalrymple & Choi, 2007; Martinius & Van den Berg, 2011). Transgressive tide-dominated systems that occur as estuaries are relatively well-studied and have robust facies models (Dalrymple *et al.*, 1992), whereas progradational tidal delta systems have received less attention in the literature. Depositional models of such environments are based on a small, but growing, set of studied ancient (e.g. Willis & Gabel, 2001; McIlroy *et al.*, 2005; Pontén & Plink-Björklund, 2007; Legler *et al.*, 2013) and modern examples (e.g. Hori *et al.*, 2002; Dalrymple *et al.*, 2003; Kuehl *et al.*, 2005). Although these examples show many similarities, they also show large differences between systems. Furthermore, the limited number of studies has led to a lack of data on geometries of depositional elements in tidal systems. These two factors present great uncertainties in forecasting hydrocarbon reservoir development of ancient deposits of tidal systems (Brandsæter *et al.*, 2005; Martinius *et al.*, 2005; Filak *et al.*, 2012).

The tide-influenced delta deposits of the Gule Horn Formation in Jameson Land, eastern Greenland, are time-equivalent and facies-equivalent to the prolific, hydrocarbon-bearing Early Jurassic Tilje Formation of the Båt Group on the Halten Terrace, offshore Norway (Dalland *et al.*, 1988; Dam & Surlyk, 1995; Martinius *et al.*, 2005; Ahokas *et al.*, 2014a; Ichaso & Dalrymple, 2014), making them an excellent analogue for these reservoirs. The Gule Horn Formation is exposed in extensive outcrops, 32 km long and 100 m thick, which are ideal for studying sedimentary architecture. A key challenge is that the outcrops are steep and largely inaccessible. To address this problem, traditional fieldwork techniques were supplemented with oblique helicopter-mounted LiDAR (light detection and ranging) scanning (Rittersbacher *et al.*, 2014), to produce large virtual outcrops which facilitate accurate collection of geobody geometries and tracing of facies boundaries and stratigraphic surfaces for improved correlation.

The goal of this work is to integrate large-scale depositional architecture, internal architecture of sedimentary bodies and fine-scale sedimentological data of a proximal, coarse-grained tide-influenced delta to increase the understanding of such systems. The aims of this study are fourfold: (i) to describe the deposits of the Gule Horn Formation in the study area; (ii) to propose a facies model for this succession which may be applicable to similar deposits elsewhere; (iii) to collect architectural data on the individual depositional elements within the tide-dominated delta succession; and (iv) to interpret how the system evolved through time under external and internal forcing factors.

GEOLOGICAL BACKGROUND

Tectonic and palaeogeographic framework

The studied outcrop occurs in cliff sections along the western side of Hurry Inlet in Jameson Land, East Greenland (Fig. 1). The deposits are of Sinemurian to Pliensbachian age (Fig. 2) and were deposited in the Jameson Land Basin which covered present day Jameson Land (Fig. 1; Surlyk, 2003).

A series of north–south elongated rift-basins formed between Norway and Greenland in the Devonian, just after culmination of the Caledonian orogeny (Surlyk, 2003). Intermittent rifting and periods of thermal subsidence continued in these basins until the Middle Jurassic. The Jameson Land basin is the southernmost of these basins, and it contains an up to 15 km thick package of sedimentary rocks (Larsen & Marcussen, 1992). The basin has been interpreted to have been in a thermally subsiding post-rift stage during deposition of the studied interval, because the succession shows overall layer-cake geometry without synsedimentary faulting or major lateral changes in thickness (Surlyk, 2003).

Volcanism in the latest Palaeocene to earliest Eocene, associated with the North Atlantic break-up, led to widespread doleritic intrusions and thick extrusions in the Jameson Land Basin and surrounding areas (Larsen & Marcussen, 1992). The extrusives are eroded in Jameson Land today, but the intrusive rocks appear as *ca* 2 m wide dykes and *ca* 9 m thick sills, which are especially common in the southern part of the study area. Two to three kilometres of uplift from the late Palaeocene until present time (Mathiesen *et al.*, 2000) led to the excellent exposures seen today (Fig. 3).

The Jameson Land Basin was located at around 45°N in the Rhaetian (Latest Triassic) and drifted northward to 50°N in the Hautervian (Early Cretaceous) (Smith *et al.*, 1994). A major

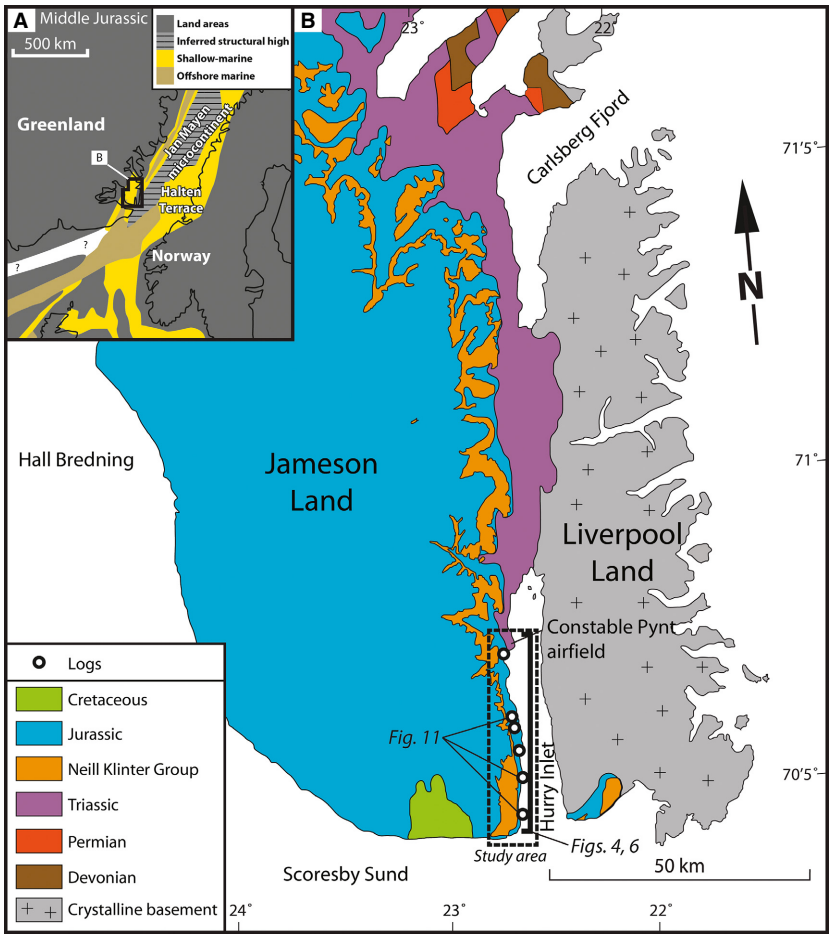

Fig. 1. (A) Schematic, pre-drift reconstruction of the seaway between Norway and Greenland in the Middle Jurassic, based on plate-tectonic reconstructions by Ziegler (1988) and Doré (1992). Note that Liverpool Land is attached to a larger landmass than today. Modified from Surlyk (2003). (B) Geological map of Jameson Land and Liverpool Land showing the outcrop of the Neill Klinter Group and the location of the study area. Modified from Ahokas *et al.* (2014a).

climatic change from arid to humid subtropical occurred at the Norian–Rhaetian transition (late Triassic), recorded by a change from red beds to lacustrine sediments (Surlyk, 2003). Palaeomagnetic data suggest that this was caused mainly by northward drift of the Laurasian continent, out of the arid subtropics into more humid latitudes (Smith *et al.*, 1994; Nystuen *et al.*, 2014). The oldest sediments exposed in the study area are lacustrine sediments of the Kap Stewart Group (Dam & Surlyk, 1993). Lacustrine conditions ended at the Sinemurian–Pliensbachian transition when the area underwent marine transgression and deposition of the shallow-marine, tide-dominated Neill Klinter Group (Dam & Surlyk, 1998).

Depositional and stratigraphic framework

Following the transgression of the lacustrine Kap Stewart Group in the upper Sinemurian (Fig. 2), the Jameson Land Basin became connected to the narrow (1500 km long and 250 km wide) seaway between Norway and Greenland (Fig. 1A), which today is represented by a tide-influenced and wave-influenced marine Jurassic succession on the mid-Norwegian shelf (Gjelberg *et al.*, 1987). In the southern Jameson Land Basin, this transgression led to deposition of transgressive shorefaces of the Rævekløft Formation. The Rævekløft Formation is overlain by the Gule Horn Formation, which was deposited by a tide-dominated shallow-marine system (Dam & Surlyk, 1998; Ahokas *et al.*, 2014a). This formation is divided into the Elis Bjerg and Albuen members (Fig. 2; Surlyk *et al.*, 1973; Dam & Surlyk, 1998). The Elis Bjerg Member consists of mainly heterolithic, thin-bedded sandstones and mudstones, cross-bedded sandstones with mud drapes on foresets and mud pebble conglomerate (Dam & Surlyk, 1998). The overlying Albuen Member consists mainly of alternating mudstones and well-sorted, wave-rippled sandstone beds and occasional massive beds with quartzitic pebbles and sparse granite boulders (Dam & Surlyk, 1998). Dam & Surlyk (1998) interpreted the Elis Bjerg Member to be deposits of a tide-dominated, shallow-marine environment, over-

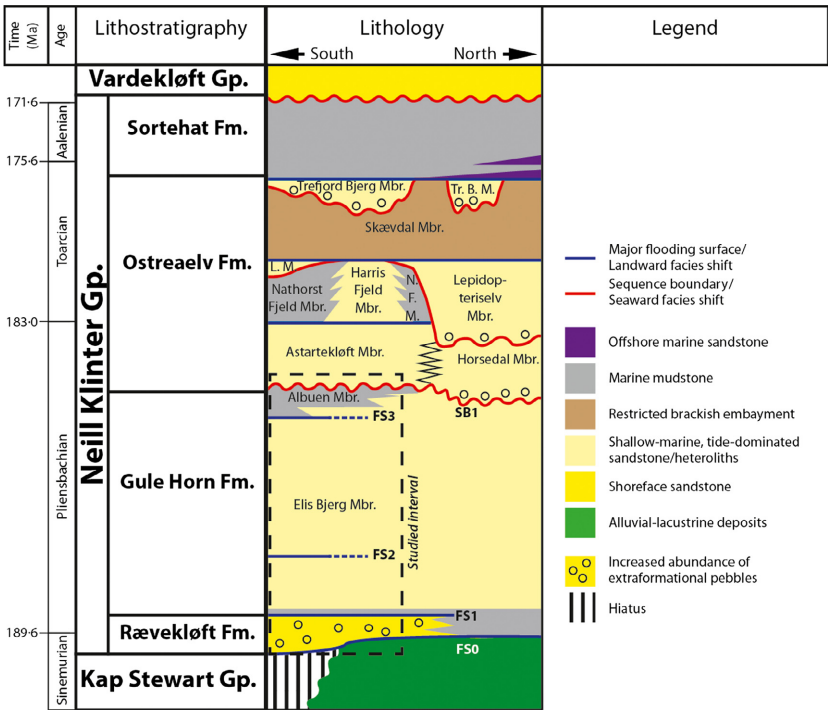

Fig. 2. Lithostratigraphical subdivision of the Neill Klinter Group. Dashed box shows location of the study interval. Modified from Ahokas *et al.* (2014a). Gp., Group; Fm., Formation; Mbr., Member; L. M., Lepidopteriselv Member; N. F. M., Nathorst Fjeld Member; Tr. B. M., Trefjord Berg Member.

lain by a major sequence boundary. The overlying Albuen Member was interpreted to be lower shoreface or prodelta deposits formed during transgression and highstand. In contrast, Ahokas *et al.* (2014a) interpreted the Elis Bjerg Member to be prograding to retrograding tide-dominated delta deposits, and the boundary with the overlying Albuen Member to reflect gradual transgression of the shallow-marine system. The Albuen Member thins significantly from south to north and pinches out a few kilometres north of the study area (Fig. 2).

The Gule Horn Formation is sharply overlain by the Astartekløft Member of the Ostreaelv Formation, which mainly consists of cross-bedded sandstones with mud-draped foresets within the study area (Dam & Surlyk, 1998). This has been interpreted as deposits of a sharp-based distributary system formed after a major sea-level fall (Ahokas *et al.*, 2014a,b). A major sea-level rise in the Aalenian led to flooding of the entire shallow-marine system of the Neill Klinter Group, and deposition of dark, offshore mudstones of the Sortehat Formation in the restricted Jameson Land Basin embayment (Fig. 2).

METHOD AND DATASET

This study documents a 32 km long, north–south-trending outcrop belt near the eastern margin of Jameson Land (Fig. 1). The dataset comprises a set of six measured sections (648 m cumulative length) and a photorealistic virtual outcrop model of the investigated outcrop acquired using oblique helicopter-mounted LiDAR scanning. This model captures the exposed part of the Neill Klinter Group below the Sortehat Formation (Fig. 3). The measured sections span the 100 to 124 m thick Gule Horn and Rævekløft formations, and in most locations also the transition into the overlying Astartekløft Member of the Ostreaelv Formation (Fig. 2). The measured sections record grain size, sedimentary structures, nature of bed contacts, sand/mud-ratio, degree of bioturbation [bioturbation index (BI), *sensu* Taylor & Goldring, 1993] and palaeocurrent directions of dune foresets.

The studied outcrop belt has been divided into five areas, labelled A to E from north to south (Fig. 3), separated by cross-cutting scree-covered intervals or canyons. At least one logged section was acquired in each area.

The dataset documents a single two-dimensional cross-section, with limited three-dimensional control provided by gullies and valleys that cross-cut the main outcrop belt. Faults are rare in the section, and tectonic dip is gentle (on average 3° towards the west). In the southernmost 20 km, the section is intruded by abundant Palaeogene dolerite sills (Larsen & Marcussen, 1992) that mainly follow mudstone units but

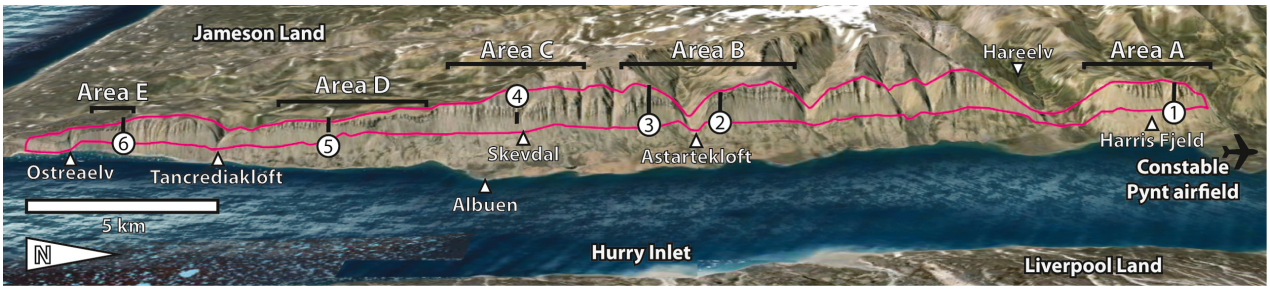

Fig. 3. Overview of the study area. Purple outline shows extent of LiDAR data and the outcropping Neill Klinter Group, and black vertical lines show location of measured sections. The 8 km section between Areas A and B is generally covered by scree and has not been studied. Scale varies in this oblique figure, and the scale bar applies to the vertical cliffs along Hurry Inlet; 3× vertical exaggeration, view from the east. Map data © Google 2013.

often cross-cut bedding and change stratigraphic interval over kilometres. Dolerite dykes are present throughout the study area, but are more widely spaced towards the north. Although earlier works (Dam & Surlyk, 1995, 1998; Ahokas *et al.*, 2014a) previously logged sections through these outcrops, the virtual outcrop model constructed for this study makes it possible to trace stratigraphic packages and correlate stratigraphic surfaces with greater confidence, to map architectural elements and larger bodies along the cross-section and to characterize the hierarchy of erosional bounding surfaces.

Acquisition and processing of LiDAR data

Virtual outcrop models (Enge *et al.*, 2007; Buckley *et al.*, 2008a) are 3D computer models of an outcrop surface textured with high-resolution digital images. The dataset used in this study was acquired using the Helimap System (Vallet & Skaloud, 2004) with a medium-format digital camera and a 35 mm lens. The distance between the outcrop face and the scanner was 300 to 400 m during data collection, resulting in a distance of around 0·3 m between measured points and an image pixel resolution of around 7 cm. The workflow for generating virtual outcrops from oblique helicopter-based LiDAR scanning is described by Buckley *et al.* (2008a) and Rittersbacher *et al.* (2014).

The raw point data are filtered to remove noise before points are triangulated to create a meshed 3D model, which the images are finally draped upon. This process results in a photorealistic, geo-referenced virtual outcrop model which can be interpreted in the office using a personal computer. Because sedimentary structures and grain size cannot be measured directly from the virtual outcrops, lithological variations observed in the measured sections are related to bedding defined by geometry and colour variation of the outcrop face. Sandstone beds appear as beige to light grey, whereas mudstones are dark grey to black. Dolerite intrusions are dark brown, resistant bodies cross-cutting bedding.

OVERALL ARCHITECTURE AND DEGREE OF EXPOSURE

The studied deposits of the Gule Horn Formation occur in a steep, north–south-trending outcrop belt with variable degree of exposure and five cross-cutting valleys (Figs 3 and 4). Parameters such as lithology, bedding, architecture and type of facies association are visually apparent in areas of good exposure (c.f. Fig. 4A). In areas of poor exposure, large-scale vertical changes in sandstone content can be inferred from slope breaks and weathering profile, facilitating recognition of

Fig. 4. Sedimentary architecture in studied outcrop, showing stratigraphic surfaces and facies associations. (A) Overview of the entire study area. Note that there is some distortion of architecture due to uplift of host rock above sills. Locations of panels (B) to (E) are indicated. RK, Rævekløft Formation; EB, Elis Bjerg Member; ALB, Albuen Member; AK, Astartekløft Formation. (B) Area E. Note the upward increase in sand content towards the top of the Elis Bjerg Member and the lack of any significant erosion surfaces below the SB1. (C) Area D. Note the abundant erosive channel geometries of FA5. (D) Area B. (E) Area A. Note the lateral terminations of FA6 (distributary channels) in the middle part of Elis Bjerg.

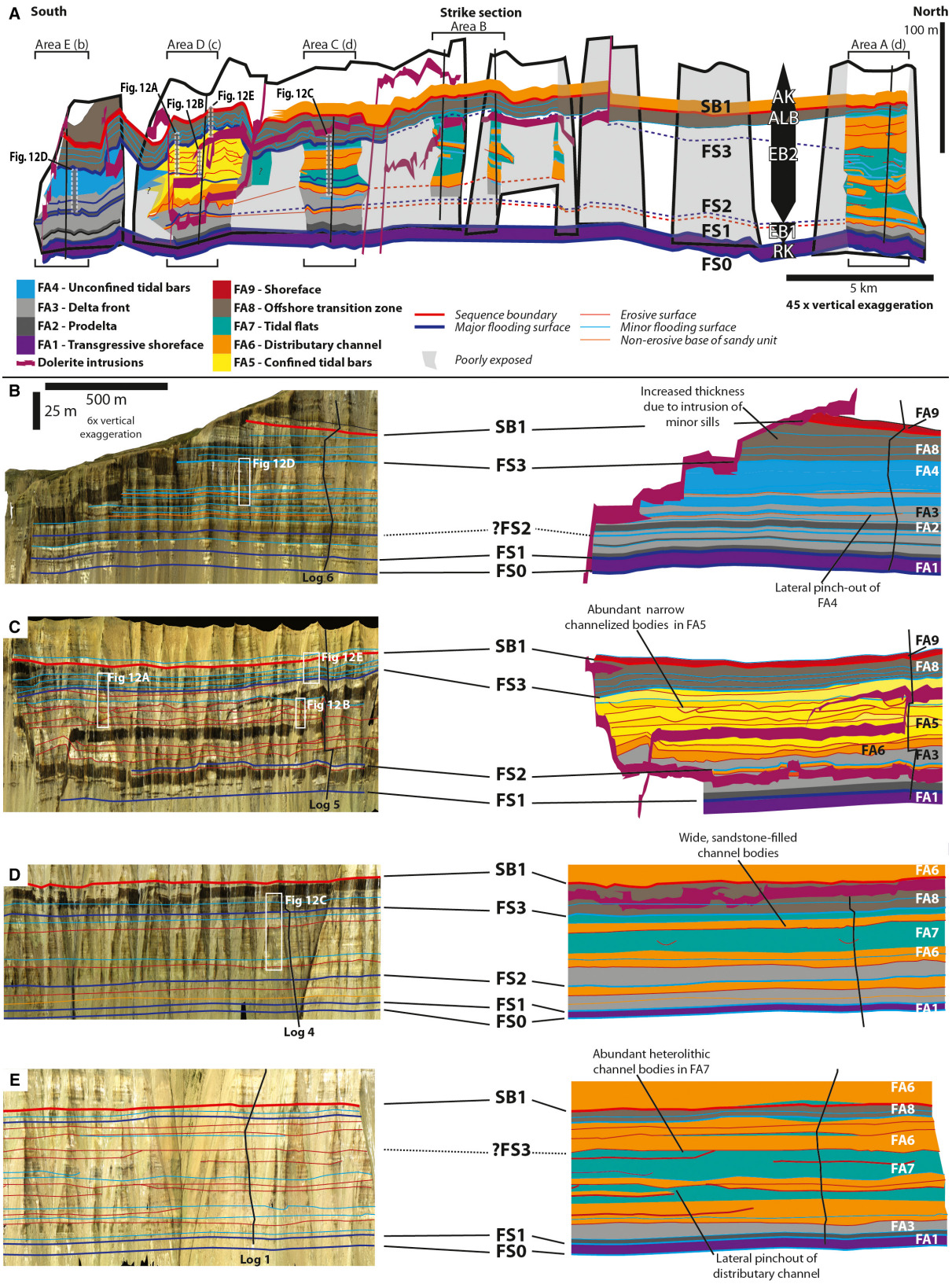

major changes in sandstone content coincident with stratigraphic boundaries, but types of facies associations and internal architecture may not be recognized. Dolerite sills occur within the sedimentary rocks. The host-rock deformation due to emplacement of intrusions is limited to vertical uplift above sills, and the reconstruction of original sedimentary geometries is generally straightforward (for example, Fig. 4C).

Palaeocurrents were measured from dune foresets in outcrop and from clinoform foresets in the virtual outcrop model (Fig. 5). These are dominantly westward-directed and indicate basinward sediment transport. This implies that the outcrop panel is a strike section. This interpretation is consistent with provenance data, which shows that the sediment was sourced from nearby Liverpool Land (Slama *et al.*, 2011; Fig. 1B).

Stratal geometries interpreted from the outcrop model are presented in Fig. 4, and a panel showing logs and correlations is presented in Fig. 6. The studied deposits are divided into five units based on large-scale trends in sandstone content.

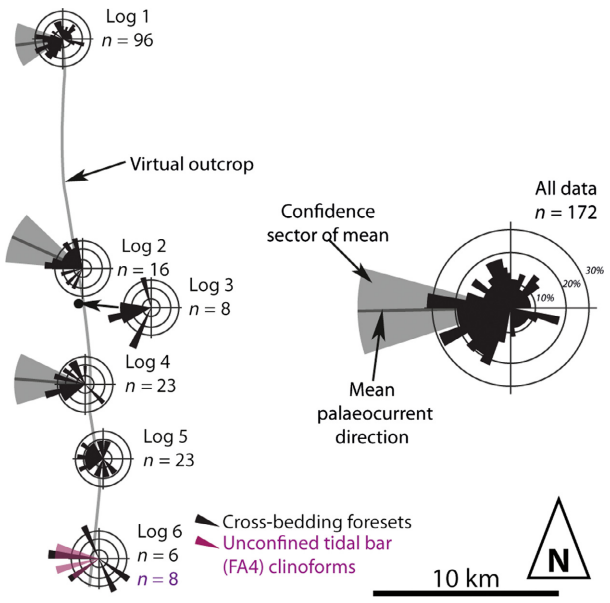

Fig. 5. Distribution of palaeocurrent measurements, based on observation of cross-bed foresets (black) observed in outcrop and unconfined tidal bar (FA4) clinoform dip directions (purple) identified in virtual outcrops. Grey sectors show confidence interval for the mean palaeocurrent direction, and the black line in the middle of these sectors shows mean palaeocurrent direction (Baas, 2000). These are not calculated in datasets that are not circular normal distributed (log 5) or have fewer than 15 measurements (logs 3 and 6). Westward palaeocurrents are interpreted as ebb-oriented currents, while eastward palaeocurrents are interpreted as flood-tidal currents. Dominance of westward-directed currents indicates that the system is an ebb-dominated system.

Rævekløft Formation

A tabular, well-cemented, *ca* 8 m thick sandstone body is present between the Kap Stewart Group and the Gule Horn Formation over the entire study area (Fig. 4A). The base represents the marine transgression of the underlying alluvial–lacustrine unit, and the top of the unit represents further deepening of the study area during the marine incursion into the Jameson Land Basin. This unit comprises the Rævekløft Formation (Fig. 2) and is interpreted as the product of transgressive reworking of the underlying alluvial–lacustrine environment (Dam & Surlyk, 1998).

Elis Bjerg 1

This is a *ca* 15 m thick, upward-coarsening unit which consists of mudstone-rich heteroliths in the lowermost part, sandstone-rich heteroliths in the middle part and cross-bedded, pebbly sandstones in the upper part. The upper, cross-bedded part is absent in the southernmost of the outcrop (Area E, Fig. 4). Elis Bjerg 1 (EB1) is overlain by a more mud-rich interval in all areas of the outcrop except the northernmost part (Area A, Fig. 4E), where there is no obvious candidate for a boundary between Elis Bjerg 1 and 2.

Elis Bjerg 2

This is the most variable of the studied units. In most of the study area, the lower part consists of a *ca* 15 m thick upward-coarsening deposit. This occurs in all areas except for the northernmost area (Area A, Fig. 4). In Areas A to C, the remainder of Elis Bjerg 2 (EB2) consists of large, sharp-based sandstone bodies (3 to 11 m thick, >2 km wide) that generally fine upward, encased in heterolithic deposits. In Area D, a basal upward-coarsening package is overlain by several sharp-based, channelized bodies which generally coarsen upward and are more mudstone rich than the sharp-based sandstone bodies in Areas A to C. In Area E, the upper part of EB2 consists of gradationally based, upward-coarsening heterolithic to sandy bodies which show internal westward-dipping surfaces (basinward), interpreted as clinoforms. In general, Elis Bjerg

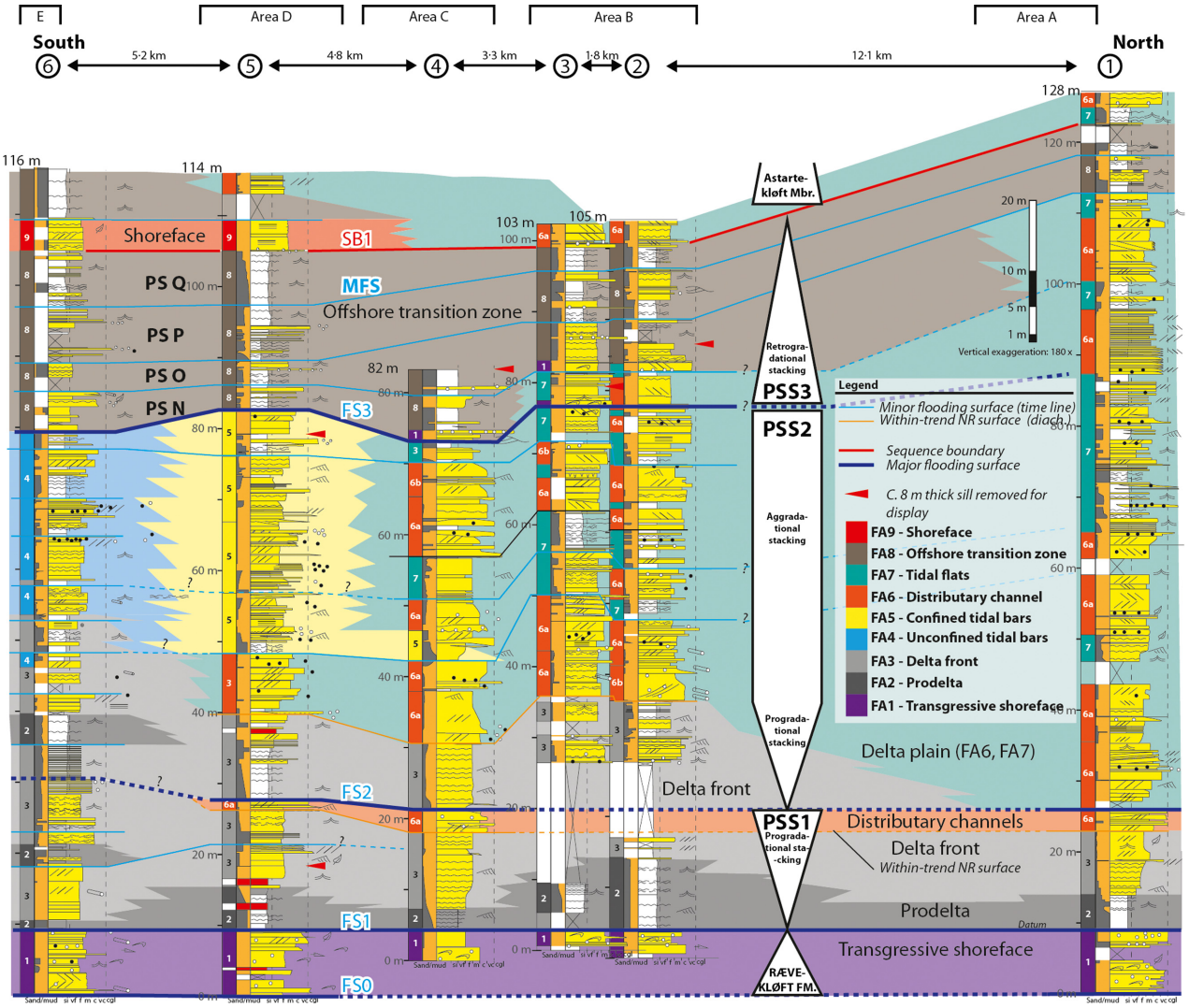

Fig. 6. Correlation panel across the study area, oriented approximately along depositional strike. See Fig. 7 for legend, and Fig. 11 for detailed view of logs 2, 5 and 6. Distance between logs is to scale. FS: Major flooding surface; SB: Sequence boundary; MFS: Maximum flooding surface; PS: Parasequence; PSS: Parasequence set.

2 exhibits a greater proportion of mudstone in the southern part than in the north.

Albuen Member

The Albuen Member consists of tabular, upward coarsening, mudstone-rich heteroliths. This unit thins considerably from 26 m in the southern part of the study area (Area E) to 11 m in the southern part (Area A) (Figs 4 and 5). It consists of four upward-coarsening packages in the southern part and only two packages in the northern part. Furthermore, each of these packages coarsens towards the north, indicating gradual backstepping of the depositional system.

Astartekløft Member

The lower boundary of Astartekløft Member is recognized as a planar, sharp-based surface overlain by sandy facies. In the northern part of the study area (Areas A to C), it consists of several metres thick cross-bedded sandstone and sandy heteroliths, while it is more mudstone-rich in the southern part (Fig. 4).

FACIES ASSOCIATIONS

Nine facies associations that can be recognized both in measured sections and virtual outcrops were observed (Fig. 8). Interpreted depositional

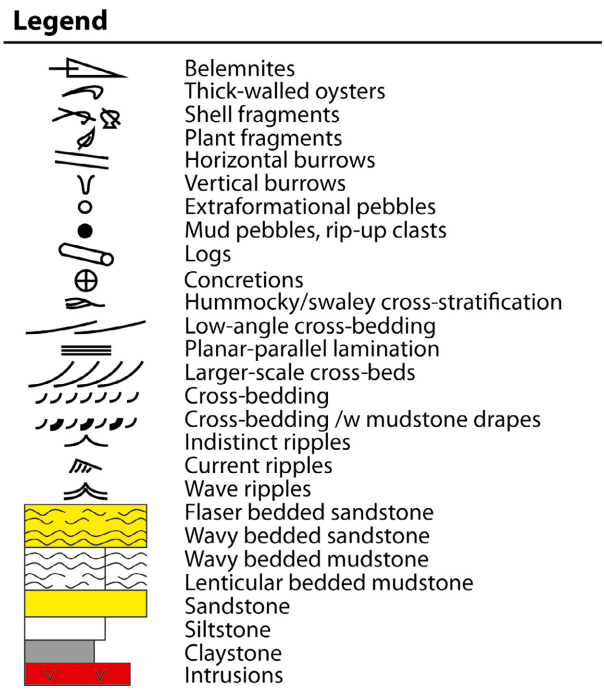

Fig. 7. Legend for stratigraphic logs and architectural cross-sections in Figs 6, 8 and 11.

environments are: Facies Association 1 (FA1) transgressive shoreface; Facies Association 2 (FA2) prodelta; Facies Association 3 (FA3) delta front; Facies Association 4 (FA4) unconfined tidal bars; Facies Association 5 (FA5) confined tidal bars; Facies Association 6 (FA6) distributary channels; Facies Association 7 (FA7) tidal flat; Facies Association 8 (FA8) wave-dominated offshore transition zone; and Facies Association 9 (FA9) shoreface. Interpreted lateral relationships and plan-view expressions of the facies associations are shown schematically in Fig. 9. Distinguishing factors of heterolithic facies associations are summarized in Table 1, and dimensions of laterally restricted facies associations are summarized in Table 2.

Facies Association 1 – Transgressive shoreface

This facies association constitutes the majority of the Rævekløft Formation, as a *ca* 8 m tabular continuous sandstone body over the entire study area. Thinner and more locally developed examples of FA1 also occur at the top of the Elis Bjerg Member, directly underlying the Albuen Member.

It consists of poorly sorted, fine-grained to very coarse-grained sandstone, with trough cross-stratification and low-angle cross-stratification, wave ripples and massive beds. It contains abundant quartzite pebbles, thick-walled bivalves, shell fragments, belemnites, plant fragments and mudstone rip-up clasts (Figs 8F, 10A to C and 11). This indicates a high-energy, marine environment. The stratigraphic position between the alluvial–lacustrine Kap Stewart Group and shallow-marine Gule Horn Formation suggests that it is a transgressive deposit. This is corroborated by the poor sorting of the deposits, the large amounts of extraformational pebbles and the presence of plant fragments, which are probably derived from the reworking of underlying deposits. Poor sorting may be related to homogenization of layers due to locally intense bioturbation. Facies Association 1 is interpreted as a transgressive shoreface deposit, with cross-stratified sandstones deposited as dunes in the shoaling wave zone and low-angle cross-beds formed as foreshore deposits (e.g. Clifton, 2006). Wavy bedding and flaser bedding might indicate some tidal influence.

Facies Association 2 – Prodelta

This facies association occurs lowermost in the Gule Horn Formation across the entire study area and also at some higher levels in the southernmost part of the outcrop (Area E). It is generally scree-covered, but is visible as dark, laterally continuous, muddy heteroliths at the base of larger coarsening-upward packages in Area E (Fig. 4).

Facies Association 2 consists of mudstone-rich heteroliths dominated by lenticular to wavy bedding with current-rippled and wave-rippled sandstone laminae and beds (Figs 8F, 10 and 11). Thin rhythmic alternations between siltstone-laminae and sandstone-laminae suggest fluctuating energy and/or sand supply and relatively slow depositional rates, with thin silt laminae settled from suspension, and thicker rippled sand beds introduced by river flood currents or storm waves. Bimodal palaeocurrents of current ripples suggest modification by tides. Upward-sandier units (<5 m thick) record local progradational events and subsequent transgression following abandonment. Relatively sparse, low-diversity bioturbation and lack of body fossils suggest a stressed, brackish environment. This probably reflects rivers debouching into a restricted marine embayment. This evidence, together with the stratigraphic occurrence of this facies association at the base of overall upward-coarsening sequences, is indicative of a prodelta environment.

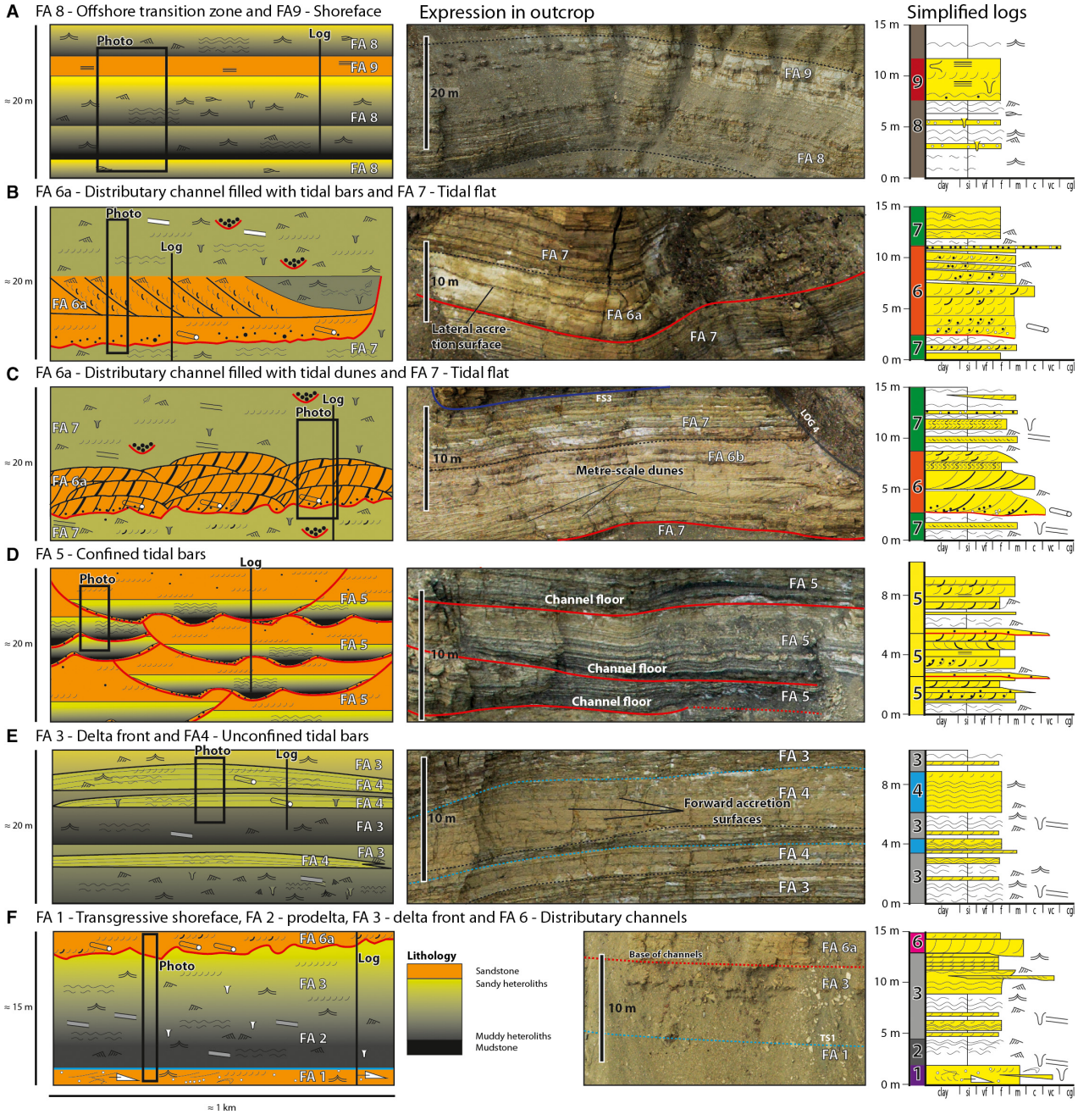

Fig. 8. Idealized expression of facies associations and their appearance in outcrop and logs. See Fig. 7 for legend. Architectural diagrams show lithology and sedimentary structures in Facies Associations 1 to 9. Black rectangles in the drawings show location of outcrop photographs, and vertical lines indicate location of idealized logs. (A) Wave-dominated shoreline deposits, FA8 and FA9. (B–C) Proxmial delta-plain, FA6 and FA7. (D) Confined tidal bars corresponding to distal delta plain, FA5. (E) Proxmial delta front deposits, FA3 and FA4. (F) Transgressive shoreface (Rævekløft Formation) and delta front deposits.

Facies Association 3 – Delta front

This facies association consists of upward-coarsening, tabular, heterolithic beds that are continuous over several hundreds of metres. Sandstone content ranges from 30 to 95%. Individual facies include: (i) wavy-bedded, fine-grained sandstone beds with current ripples and wave ripples; (ii) cross-stratified, fine-grained to very coarse-grained sandstone beds with rare mudstone drapes on foresets; (iii) lenticular

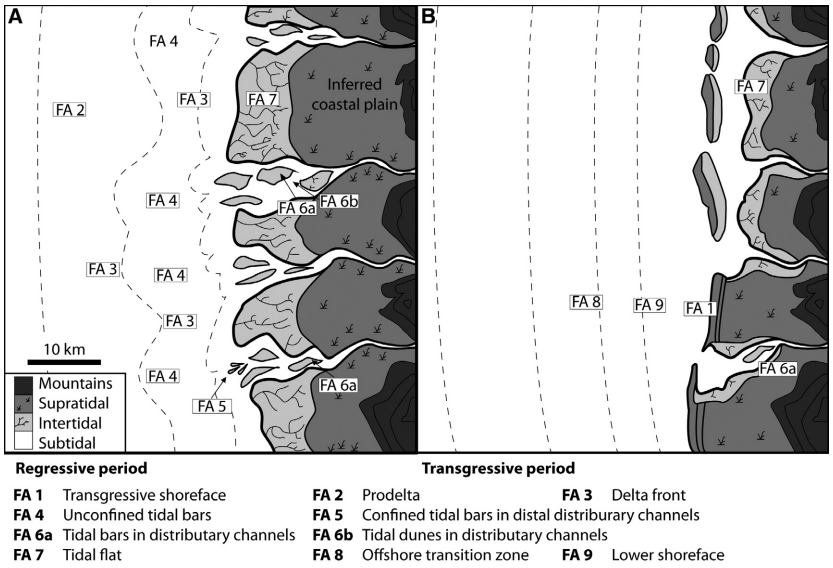

Fig. 9. Schematic map view of a tide-dominated shallow-marine sedimentary system with multiple, closely spaced distributaries, showing the lateral relationships between interpreted facies associations in the Gule Horn Formation. Supratidal deposits are inferred, because these have not been observed in the study area. Expression during a regressive period (A) and transgressive period (B).

Table 1. Comparison of heterolithic facies associations, with distinguishing features highlighted in bold type.

Facies association	Sandstone content	Wave ripples	Current ripples	Fluid mud beds	Drowning ripples	Bioturbation	Secondary characteristics
FA2: Prodelta	**Low**	Abundant	Abundant	Uncommon	Uncommon	Low–moderate	**High mud-content**
FA3: Delta front	Variable	Abundant	Abundant	Uncommon	Uncommon	Low–moderate	**Tabular beds, no associated minor channels**
FA4: Unconfined tidal bars	**High**	Abundant	Abundant	Uncommon	Uncommon	Low–moderate	**Forward accretion surfaces**
FA5: Confined tidal bars	Upward increase	Sparse	Abundant	**Thick, abundant**	**Abundant**	Low–moderate	**Basal erosion, debris flows**
FA7: Tidal flat	Variable	Sparse	Abundant	Uncommon	Sparse	Low–moderate	**Channels containing mud-pebble conglomerate and IHS**
FA8: Offshore transition zone	Low	**Abundant**	**Sparse**	Uncommon	Uncommon	Low–moderate	**Hummocky cross-stratified beds, pebbly beds**

bedded wave-rippled or current-rippled fine-grained to medium-grained heteroliths; and (iv) sandstone beds with planar-parallel lamination (Figs 8F, 10E, 10F and 11). Mudstone rip-up clasts, plant fragments and extraformational pebbles are common. Bioturbation index varies from 0 to 1.

This facies association is dominated by tractional sedimentary structures formed under unidirectional currents, with localized wave reworking. Sheet-like sandstones suggest unconfined flows. Mudstone drapes within cross-bed foresets indicate slack-water periods associated with tides. The sedimentary structures, gradational transition from the underlying muddy heteroliths, presence of marine palynomorphs (Ahokas *et al.*, 2014a) and upward-coarsening trends suggest a delta front that was modified by

Table 2. Dimensions of laterally restricted architectural elements.

Facies association	Thickness (m)	Along strike width (m)
FA4: Unconfined tidal bars	1·4–4·3	540–>1200
FA5: Confined tidal bars	3·8–12·0	80–>1500
FA6a: Distributary channel with tidal dunes	3·1–7·5	>1900
FA6b: Distributary channel with tidal bars	2·9–10·9	>4500

wave and tidal processes. Occasional very coarse-grained sandstone beds probably were deposited on the delta front during river floods.

Facies Association 4 – Unconfined tidal bars

This facies succession occurs in 1·5 to 4·3 m thick, 0·5 km to more than 1·2 km wide (wider than the exposed sections) tabular bodies. One body is observed to thin laterally and pinch out (Fig. 4B), and most bodies thin gradually from their thicker axis; they are therefore inferred to have a convex-up lenticular shape (Fig. 8E). Internal clinoformal beds dip 3° westward in some examples (Fig. 12D), and many are continuous for hundreds of metres along the cliffs. This facies is only observed in Area E in the southern part of the outcrop belt and is associated with thick delta-front deposits (FA3).

Facies Association 4 is characterized by upward-coarsening successions with gradational bases and an upward increase in sandstone content (Fig. 8A). Wavy-bedded, wave-rippled and current-rippled heteroliths occur in the lower parts, and wavy-bedded and cross-stratified fine to coarse-grained sandstone beds with mudstone draped foresets and rip-up mudstone pebbles occur in the upper parts (Fig. 13A to C). Palaeocurrents are generally towards the west (basinward). No signs of erosion or emergence were observed.

The basal, heterolithic beds were deposited during occasional bedload transport of sand, interrupted by suspension fallout of mud. The

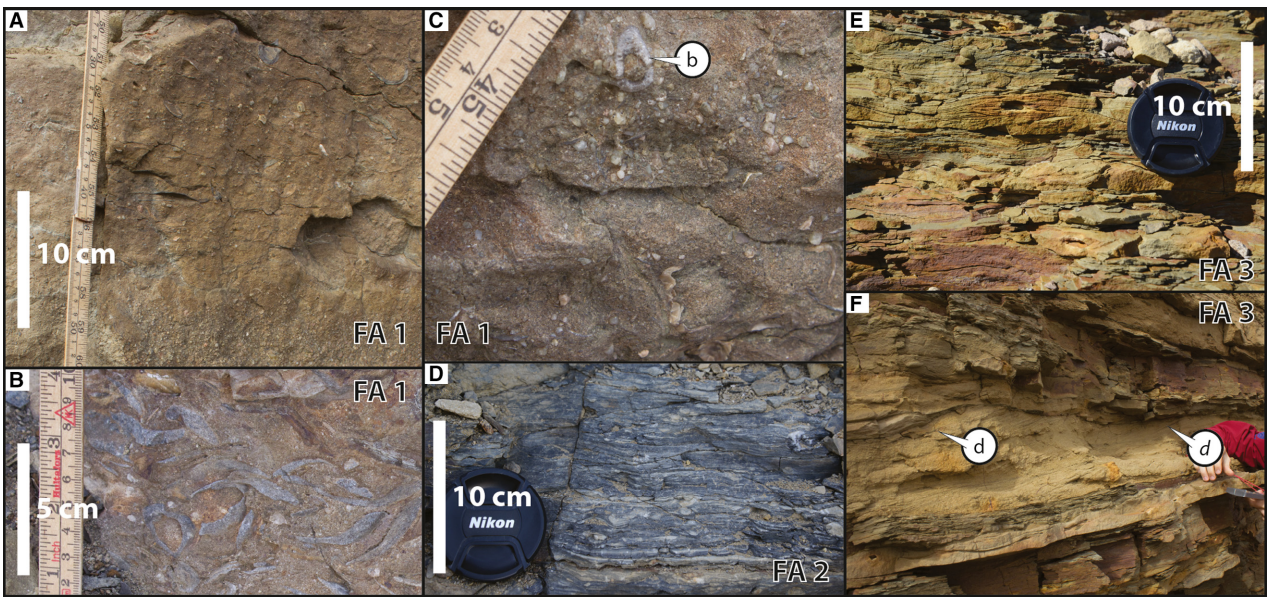

Fig. 10. Examples of facies associations 1, transgressive shoreface (A) to (C); 2, prodelta (D) and 3, delta front (E) and (F). (A) Typical expression of the Rævekløft Formation showing poorly sorted pebbly sandstone with shell fragments, belemnites and sparse organic debris. From 2·5 m in log 2. (B) Poorly sorted sandstone with abundant thick-walled bivalves. From 74 m in log 3. (C) Detail of FA1 showing belemnites (b), shell fragments and extraformational pebbles. From 1·5 m in log 2. (D) Typical deposits of FA2 (prodelta). Dark siltstone with up to 1 cm thick, wave-rippled sandstone laminae and abundant, horizontal, *Planolites* burrows. From 15 m in log 5. (E) Typical deposits of FA3 (delta front). Sand-rich heteroliths, mainly wave-rippled fine-grained sandstone with horizontal, sand filled burrows. From 17 m in log 1. (F) Typical deposits of the upper part of FA3 (delta front). Wavy-bedded, wave-rippled and current-rippled heteroliths in the top and base of the image. Middle part shows two sets of planar cross-bedded, fine-grained, poorly sorted sandstone with occasional mud drapes on foresets (d). From 36 m in log 2.

overlying cross-stratified sandstone beds with internal mudstone drapes on foresets indicate tidal currents interrupted by slack-water periods. The large width, tabular to convex upward lenticular shape, and lack of a basal erosion surface indicate that these units were deposited as unconfined sheets or bars.

Trough-going, palaeoseaward-dipping clinoforms indicate that these bodies accreted basinward upon the mostly planar delta-front deposits of FA3, which lack the forward accretion surfaces in FA4 and show a more chaotic development. Architectural relations (c.f. Fig. 4A) show that FA4 was deposited in close proximity to, and probably seaward of, tide-influenced distributary channels (FA6 and FA5). These bodies are similar to the downcurrent-accreting tidal bars described by Legler *et al.* (2013) from the Dir Abu Lifa Member in Egypt. However, the tops of FA4 are not vegetated and do not show erosion which could be attributed to subaerial exposure, and thus they appear to be fully subaqueous. Kuehl *et al.* (2005) describe interdistributary islands in the Ganges-Brahmaputra Delta with digitate subaqueous shoals that merge seaward into a broad, lobate apron on the delta front. The bodies of FA4 were probably deposited in similar setting and are likely to represent the unconfined, downstream extension of the confined tidal bars of FA5. Rounded mudstone pebbles are probably remnants of fluid mud beds eroded further upstream, subsequently transported as pebbles rolling along channel bases, because very little erosion and fluid mudstone beds are observed in FA4.

Facies Association 5 – Confined tidal bars

This facies association occurs within channelized, concave-upward erosional surfaces. Each body has a clear sandier-upward trend, with abundant dark mudstone beds in the lower part, and amalgamated sandstone beds in the upper part (Figs 4C, 8D, 12A and 12B). Beds appear to be conformal to the basal bounding surface, i.e. beds draping the channel margins are inclined, whereas beds draping the channel base are flat. This implies deposition in relatively straight channels that accreted vertically. The thickness of bodies in FA5 varies from 3·8 to 12 m, and the width ranges from 80 m to more than 1·5 km.

The basal erosion surface is directly overlain by a cross-bedded, poorly sorted coarse-grained sandstone bed with abundant extraformational pebbles and mudclasts, interpreted as basal lag deposits. This is further overlain by *ca* 1·5 m thick, dark, heteroliths consisting of homogeneous mudstone beds interbedded with current-rippled sandstones with abundant drowning ripples. This is interpreted as interlaminated ripple cross-laminations and fluid mud deposits (*sensu* Ichaso & Dalrymple, 2009) deposited during rapid settling of mud. Drowning ripples indicate that the current was still moving as the mud started to settle within an area of rapid sedimentation and high suspended mud concentration (c.f. Van den Berg *et al.*, 2007). Chaotic, coarse-grained sandstone lenses (Figs 11B and 13E to G) also occur within these lower deposits and are interpreted as deposits of debris flows caused by channel bank failures. The upper and thickest part of the facies association consists of trough cross-stratified, fine-grained to very coarse-grained sandstone beds, which often coarsen upward (Figs 11B, 13D and 13F). The cross-bed foresets commonly show single and double mud drapes, some are also draped by abundant rounded mud pebbles. Some of the cross-stratified beds have apparent cyclical variation in bundle thickness.

Facies Association 5 is interpreted to have been deposited close to the turbidity maximum of a prograding tidal delta (c.f. Dalrymple & Choi, 2007); FA5 is interpreted as deposits of confined, elongate tidal bars infilling distal parts of tide-influenced distributary channels. The upward increase in sandstone content from fluid muds at the base to amalgamated sand beds on the top is similar to what has been observed from tidal bars in tidal channels in the modern Fly River Delta (Dalrymple *et al.*, 2003) and Gironde estuary (Fenies & Tastet, 1998). However, in contrast to the tidal bars described by these authors, the bars in the Elis Bjerg Member are not overlain by intertidal marsh deposits, probably because the topsets are eroded by younger channels (c.f. the Devonian Guaja Formation described by Pontén & Plink-Björklund, 2009).

Fig. 11. Selected logs showing all facies associations described in the studied interval. See Fig. 3 for location and Fig. 7 for legend. (A) Log 6 from the most distal parts of the study area, Area E. Note the overall finer grain size compared to the two other logs. (B) Log 5 from the medial parts of the study area, Area D. (C) Log 2 from the more proximal parts of the study area, Area B.

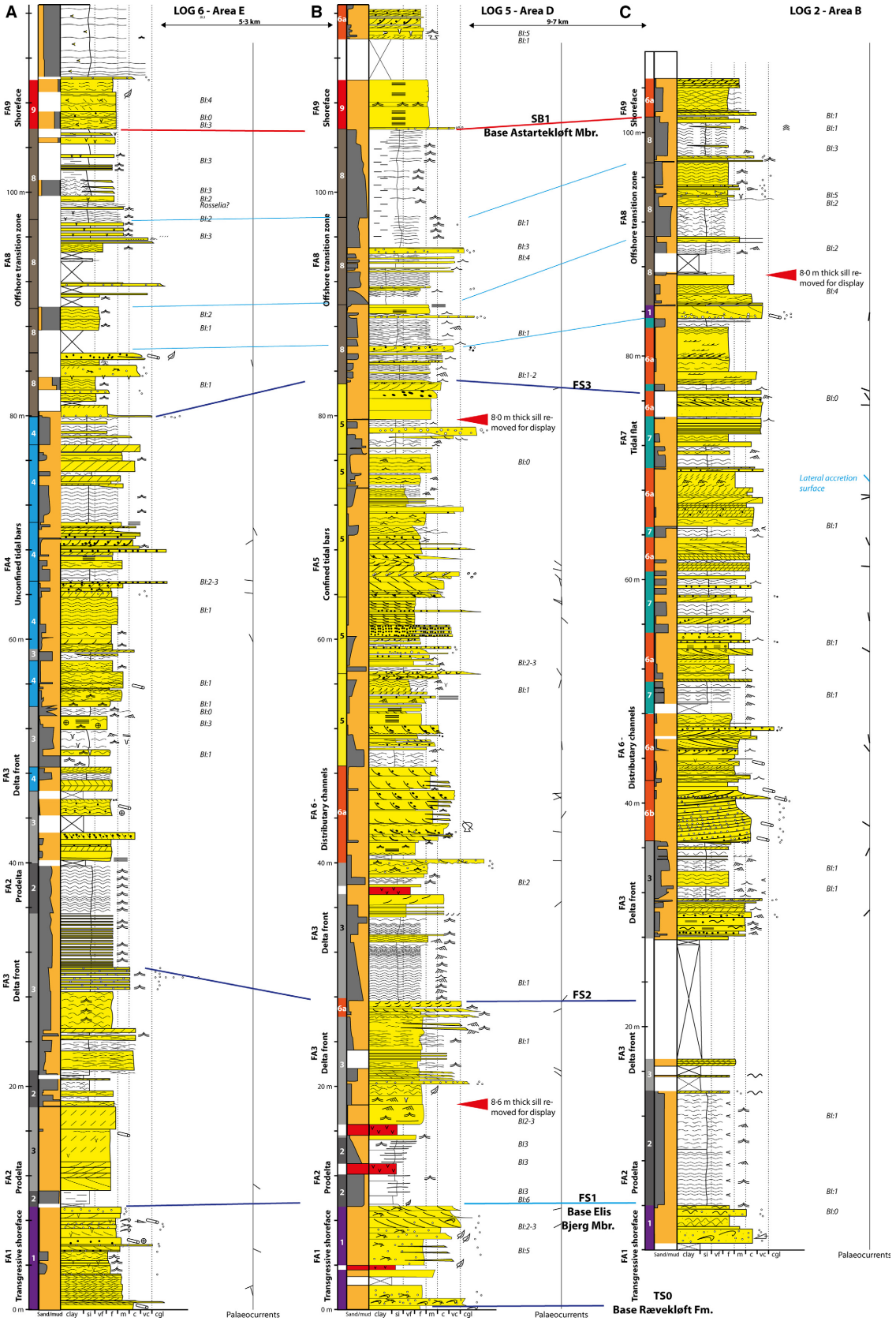
A
LOG 6 - Area E
5-3 km
B
LOG 5 - Area D
9-7 km
C
LOG 2 - Area B
SB1
Base Astartekløft Mbr.
FS3
FS2
FS1
Base Elis Bjerg Mbr.
TS0
Base Rævekløft Fm.
8·0 m thick sill removed for display
8·6 m thick sill removed for display
Lateral accretion surface
FA9 Shoreface
FA8 Offshore transition zone
FA4 Unconfined tidal bars
FA5 Confined tidal bars
FA7 Tidal flat
FA6 - Distributary channels
FA3 Delta front
FA2 Prodelta
FA1 Transgressive shoreface
Rosselia?
Palaeocurrents
Sand/mud clay si vf f m c vc cgl

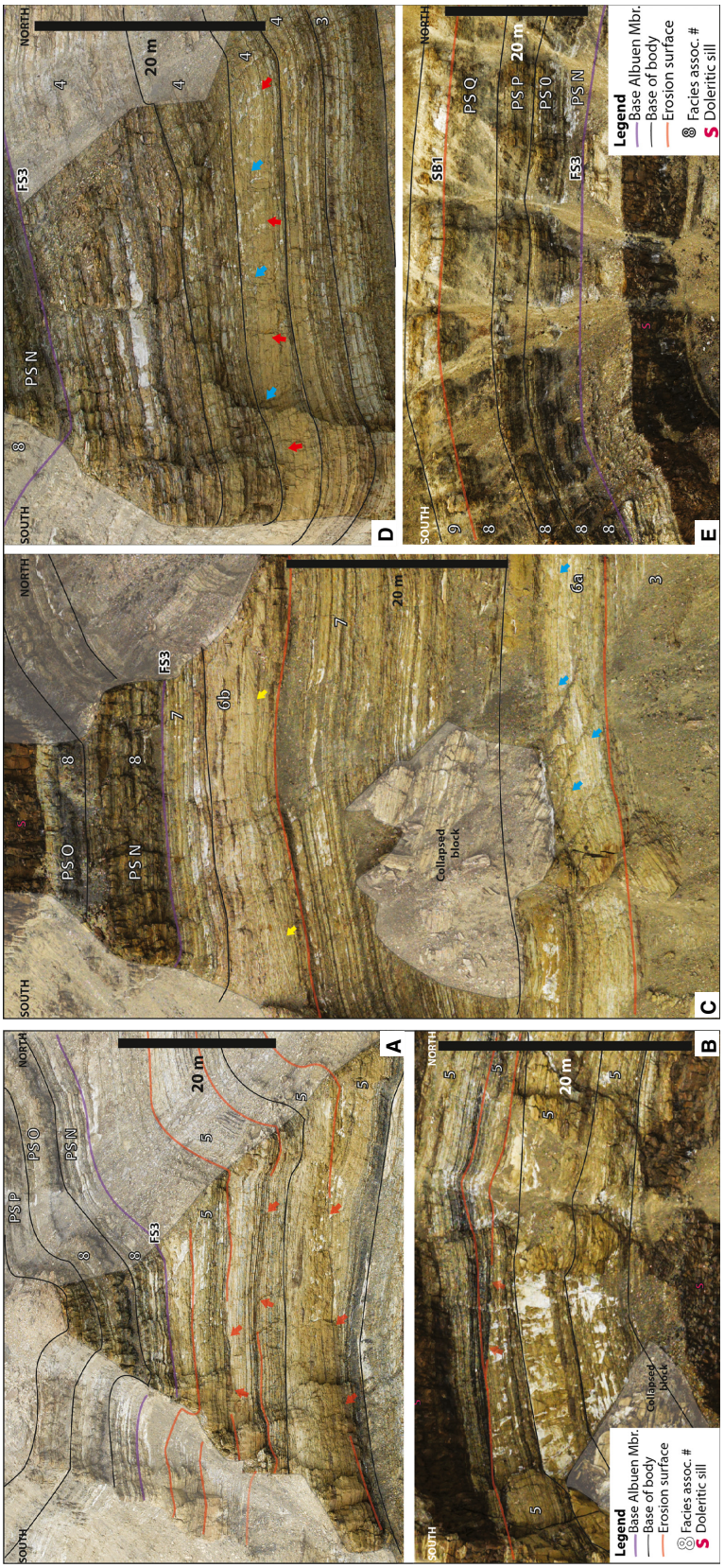

Fig. 12. Typical examples of facies associations 3 to 9 in outcrop. See Fig. 4 for location: FA1 and FA2 are not shown, because these are generally screecovered. (A) Outcrop expression of FA5 (unconfined tidal bars) and FA8 (offshore transition). In FA5, note the mudstone-rich lower parts, upward increase in sand content and the large amount of erosion at bases of bodies (red arrows). FA8 occurs as dark, mudstone rich, tabular, slightly upward-sandier units. (B) Example of FA5 (unconfined tidal bars), showing upward increase in sand content and pronounced, metre-scale erosion into underlying deposits. Erosive bases are overlain by heteroliths which are conformal to the base of channels, and no inclined heterolithic stratification is observed. This indicates vertical infilling of these channels. (C) Examples of FA6a, FA6b (distributary channels filled by tidal bars and tidal dunes, respectively), FA7 (tidal flat) and FA8 (offshore transition zone). FA6a consists of upward-fining sandbodies underlain by a low-relief erosion surface and *ca* 2° southward-dipping (normal to inferred palaeoshoreline) surfaces interpreted as lateral accretion surfaces (blue arrows). FA6b is upward-fining, underlain by a low-relief erosion surface, and contains up to 4 m thick cross-bedded sets (yellow arrows point to *ca* 1·8 m thick examples of this). FA7 consists of planar, laterally continuous heterolithic beds. FA8 shows one proximal, sandy example (PS O) and one distal, muddier example (PS N). (D) Facies associations 3 (delta front), 4 (unconfined tidal bars) and 8 (offshore transition zone). FA3 is characterized by tabular, upward coarsening and sandier heteroliths. It occasionally grades into element 4, which is dominantly sandy and contains shallowly seaward-dipping (*ca* 2°) surfaces (red and blue arrows), interpreted as forward accretion surfaces. (E) FA8 and FA9. FA8 occurs as tabular, upward-sandier heteroliths which can be traced for very large distances. FA9 occurs as a tabular sandstone body.

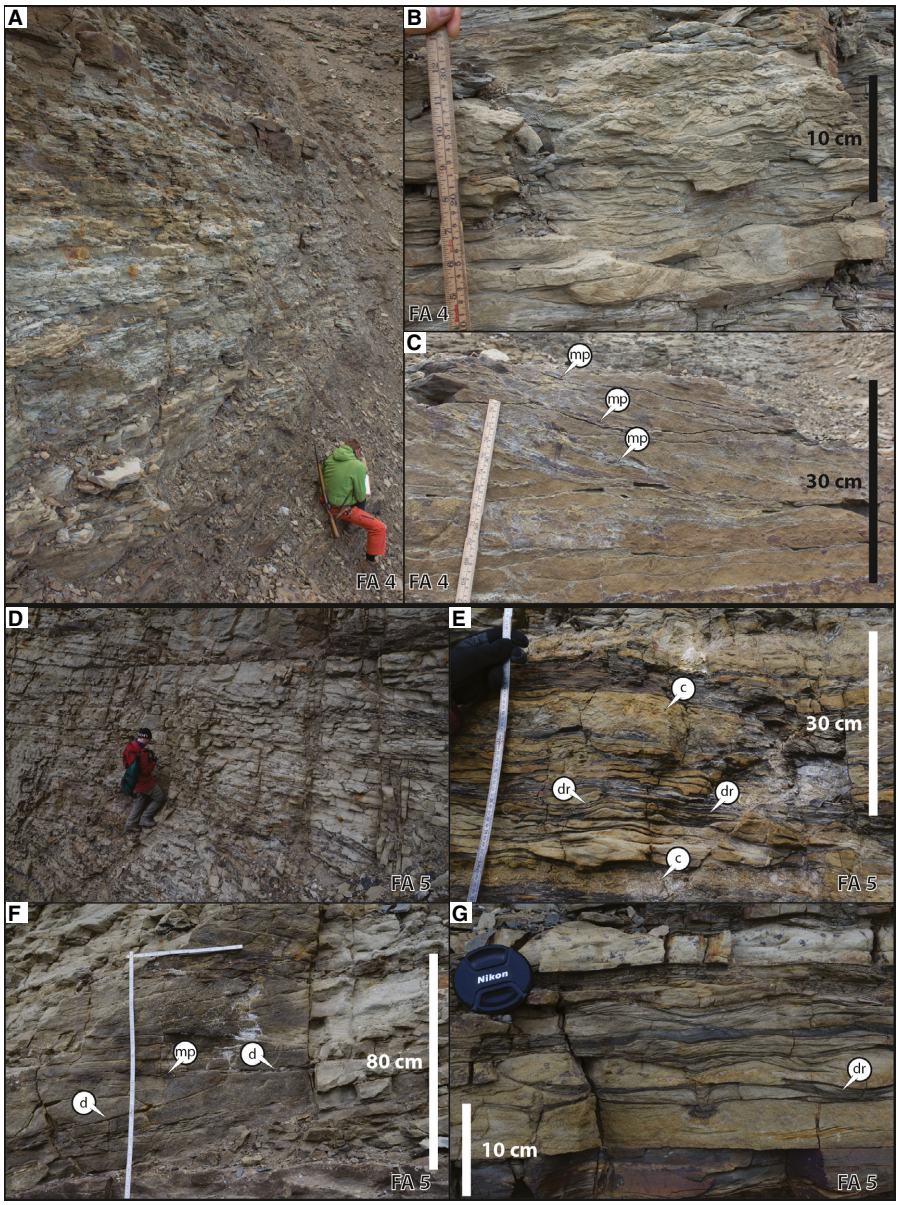

Fig. 13. Facies associations 4, unconfined tidal bars (A) to (C); and 5, confined tidal bars (D) to (G). (A) Overview of distal FA4. Upward-coarsening heteroliths consisting 5 to 10 cm thick siltstone beds with thin sandstone beds and laminae, and occasional 1 to 20 cm thick, wave-rippled and current-rippled and planar-parallel laminated sandstone beds. From 48 m in log 6. (B) Detail of medial part of FA4: Sand-rich, somewhat bioturbated (BI: 1 to 4) heteroliths of FA4, mainly displaying wave ripples. From 56 m in log 6. (C) Proximal example of FA4: Reddish, well-cemented, tangential cross-bedded, fine-grained sandstone beds with mud pebbles (mp). From 47 m in log 6. (D) Upper, sandstone-dominated part of FA5: Lower half of image shows stacked 20 to 40 cm thick cross-bedded fine-grained sandstone beds, separated by *ca* 1 cm thick siltstone beds with local horizons rich in mud pebbles. Upper half consists of coarse-grained to very coarse-grained cross-bedded sets up to 75 cm thick with occasional mudstone drapes on foresets. Person for scale is *ca* 1·7 m tall. From 68 m in log 5. (E) Lower, mudstone-rich part of FA5: Mixed, wavy to lenticular bedded heteroliths. Fine-grained sandstone beds are 1 to 3 cm thick and display slightly wave-modified, bidirectional current ripples and occasional drowning ripples (dr). Interstitial mudstone beds appear homogeneous, indicating that they are fluid mud deposits, deposited during one slack-water period. Chaotic beds (c) interpreted as debris flows, possibly related to bank failures. From 59 m in log 5. (F) Detail of upper part of FA5: Three sets of tangential cross-bedded fine-grained sandstone with mudstone drapes on foresets (d) and occasional mud pebbles (mp). From 67 m in log 5. (G) Medial part of FA5: Sandy heteroliths with relatively thick sandstone beds, bidirectional current ripples, fluid mudstone beds and drowning ripples (dr). From 56 m in log 5.

Facies Association 5 shows a similar, upward-coarsening motif to FA4, which it occurs close to and probably up depositional dip from (Figs 6 and 9); FA5 is distinguished by the high-energy sedimentary structures and concave upward erosion surfaces that the bodies are contained within, while FA4 occurs as tabular to convex upward units. This indicates that FA5 represents confined tidal bars prograding within straight channels, while FA4 represents unconfined bars prograding on the delta front.

Facies Association 6 – Distributary channels

This facies association consists of fine to coarse-grained, trough cross-stratified sandstone beds with frequent mudstone drapes on cross-bed foresets (Fig. 8B and C). Bodies of this association are several kilometres wide and never confined by the studied outcrops (Fig. 4B to D). The internal architecture is variable, and it has therefore been divided into two subdivisions: (i) Facies Association 6a (FA6a) contains lateral accretion sets composed of cross-bedded sets thinner than 1 m; and (ii) Facies Association 6b (FA6b) contains forward accretion sets thicker than 1 m. Both are commonly underlain by relatively planar erosion surfaces with relief up to 0·5 m. This erosion surface is commonly overlain by logs, plant fragments, mud pebbles and extraformational clasts, and the deposits generally fine upward. Palaeocurrents are dominantly basinward directed. No lateral cut banks or concave-upward erosional surfaces were observed associated with these deposits, except for one sandstone body that terminates laterally by interfingering with FA7 in the northernmost outcrop. The thickness of these bodies ranges from 2 to 10 m.

Abundant mudstone drapes and occasional set-climbing ripples occur on generally seaward-directed cross-beds in FA6. These indicate ebb-directed dominant tidal currents, slack-water periods and a much weaker flood-directed current relative to the ebb-directed flow (Visser, 1980). Low abundance of simple burrows and large cross-bed size indicate a stressed, brackish, high-energy environment. The basal erosion surfaces, upward fining and clast-rich bases indicate flow in channels, with the coarsest sediment being located in the channel thalwegs. These are, therefore, interpreted to be the deposits of tide-influenced distributary channels on the delta plain. The large width of these bodies is interpreted to reflect that they were very wide and/or migrated widely, as is reported from many ancient and modern tide-dominated marginal systems (e.g. Dalrymple *et al.*, 2003; Hubbard *et al.*, 2011) where distributary channels are several kilometres wide and channel migration rate is rapid.

Facies Association 6a – Distributary channel filled by tidal bars

Very gently dipping (1 to 2°) internal bedding surfaces, which are oriented normal to overall sediment transport, are visible in FA6a in Areas B and C (Figs 8B and 12C). These are interpreted as lateral accretion surfaces. The lower part of FA6a consists of stacked coarse to fine-grained, trough cross-stratified sandstone beds generally thinner than 1 m, with abundant single or double mud drapes; sparse oppositely directed current ripples; and occasional mud-pebble conglomerate on foresets (Figs 8B, 8C and 14A to C). The upper parts commonly consist of slightly inclined, trough cross-stratified fine- to medium-grained sandstone beds with carbonaceous drapes on the foresets, interbedded with up to 10 cm thick, lenticular to wavy-bedded mudstone beds, or draped by mud-pebble conglomerate. Lateral accretion surfaces, abundant tidal indicators, an upward fining motif indicates deposition as tidal bars in tidal channels. No instances of both edges of any one of these channels are observed, and single edges are only observed in Area A (Fig. 4E), which could indicate that the channels become narrower in proximal areas. This is consistent with observations of both seaward flaring channels, and a zone of rapid channel migration located at the bedload convergence zone, often observed in modern tide-dominated systems (Dalrymple & Choi, 2007).

Facies Association 6b – Distributary channels filled by tidal dunes

This facies association consists of erosively based sandstone bodies, containing 1 to 4 m thick cross-bedded sets of fine to coarse-grained sandstone, which fine upward (Figs 8C and 11B). The foresets dip basinward with dips close to 23°. They comprised rhythmic, normal-graded, 2 to 5 cm thick beds with grain sizes ranging from very coarse-grained to medium-grained sandstone (Fig. 14D). Some of these beds are separated by thin, discontinuous mudstone drapes. The normal-graded beds and sparse mudstone drapes are interpreted as the result of tidal modulation of the river flow and sparse slack-water periods. The lack of any

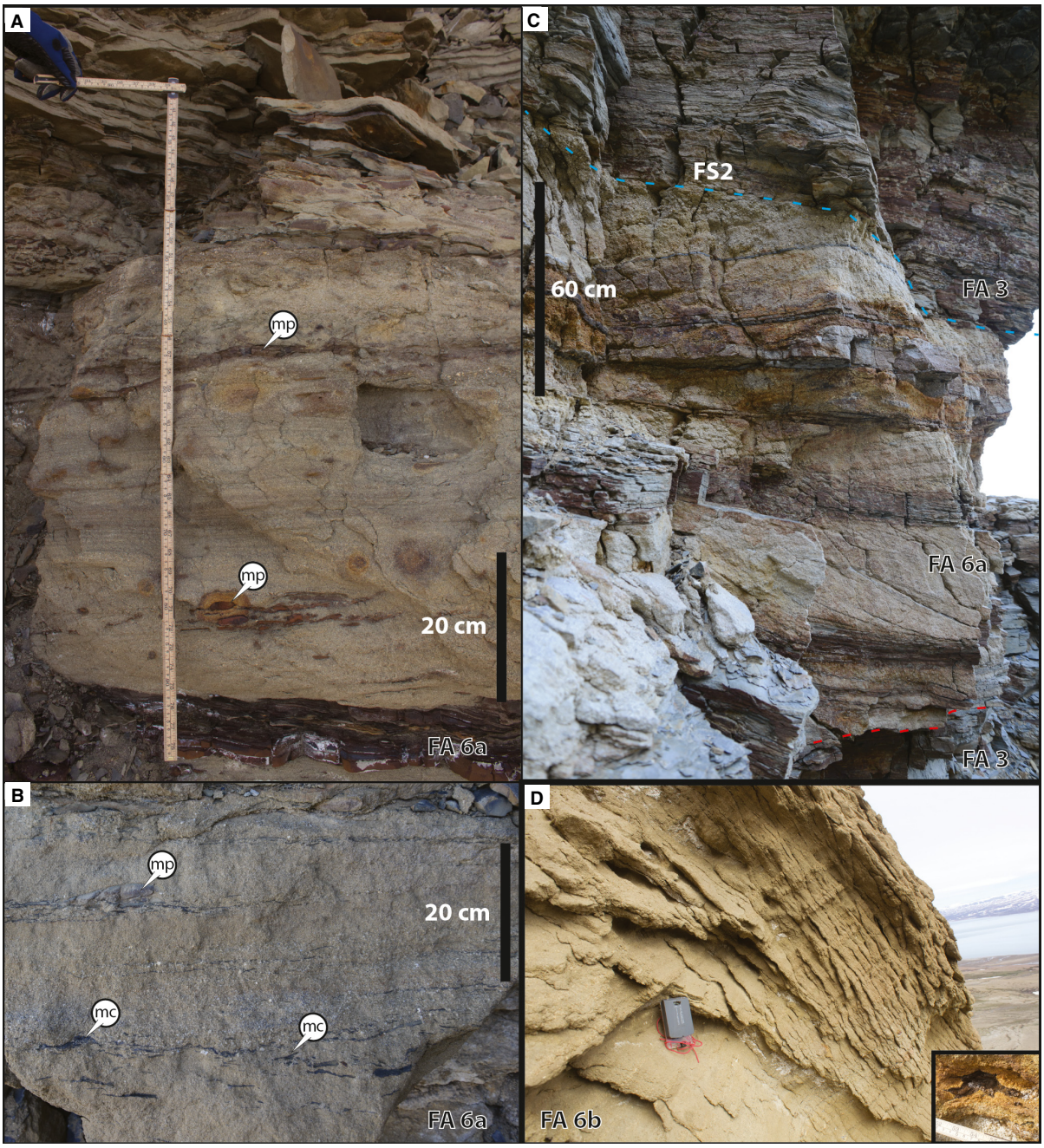

Fig. 14. Facies Association 6, tide-influenced distributary channels. (A) FA6b: Low-angle cross-bedded medium-grained, poorly sorted, pebbly sandstones with abundant mud pebbles (mp). Occasionally draped by 5 cm thick mudstone beds. Interpreted as tidal bar deposits. From 46 m in log 3. (B) Cross-bedded, medium-grained to very coarse-grained sandstone bed with abundant mud chips (mc) and mud pebbles (mp) on some foresets. From 43 m in log 5. (C) 20 to 40 cm thick tangential cross-bedded, coarse-grained to very coarse-grained sandstone beds with rippled, muddy toesets and mudstone drapes on foresets. Stippled blue line is the FS2, overlain by distal delta-front deposits (FA 3). The stippled red line marks erosion of FA6 into FA3. From 27 m in log 5. (D) FA6b: Part of a single, 4 m thick cross-bedded set. Modal grain size is coarse sandstone, foresets are composed of 2 to 5 cm thick normal graded cycles spanning medium to very coarse sandstone. Foresets record basinward transport and dip with an angle of 23°. Contains abundant mud pebbles, quartzite pebbles and organic fragments. Inset picture shows an 8 cm long woody fragment. From 38 m in log 2. Compass for scale (10 cm long).

oppositely directed ripples on the foresets indicates a very weak subordinate current in relation to the dominant ebb-directed current (e.g. Martinius & Van den Berg, 2011). Facies Association 6b is interpreted as deposits of simple and compound tidal dunes (Ashley, 1990) because of the scale of the cross-bedding, evidence for tidal modulation and the interpreted forward migration of the bedform (c.f. Olariu *et al.*, 2012). The large scale of the dunes (1 to 4 m) indicates that they formed in relatively deep water and may, therefore, represent the deeper thalwegs of tide-influenced distributary channels.

Facies Association 7 – Tidal flat

This facies association occurs as planar and continuous heterolithic beds (Fig. 12C). It mainly consists of wavy-bedded heteroliths with thin current-rippled sandstones occasionally showing drowning ripples, relatively thin, laterally discontinuous, fine-grained to coarse-grained cross-stratified sandstone beds, with abundant mud drapes on foresets (Figs 8B, 11B, 11C and 15A). This facies association also contains three types of isolated bodies: (i) laterally restricted (50 to 200 m wide) deposits of inclined heterolithic stratification (IHS, *sensu* Thomas *et al.*, 1987; Fig. 13C) with an inclination of *ca* 5°; (ii) *ca* 10 m wide and up to 0·5 m thick, erosionally based lenses of mud pebble conglomerate (Fig. 13B); and (iii) more than 200 m wide, 2 m thick bodies consisting of darker mudstones with thin, wave-rippled sandstone beds. Bioturbation is generally of low intensity and diversity, with a bioturbation index ranging from 0 to 3, but a few beds are observed to be completely reworked by *Diplocraterion* burrows. The sand content ranges from 0 to 100%, but is on average near 50%.

The lithology and sedimentary structures of this facies association are similar to the delta-front deposits of FA3 (c.f. Storms *et al.*, 2005), but does not show an upward-coarsening trend, and contains well-defined, minor channels which are absent in FA3. The planar, continuous geometries, evidence for tides and presence of minor erosional channels lead to an interpretation as tidal flats. The facies association lacks evidence for subaerial exposure, such as desiccation cracks, coal beds or rootlets, and is therefore interpreted to have been deposited in the subtidal to lower intertidal zone. Small IHS bodies, up to 10 m wide mud–pebble–conglomerate-filled channels and laterally restricted mudstone bodies are interpreted as deposits of tidal creeks which drained the tidal flats.

Facies Association 8 – Offshore transition zone

This facies association consists of tabular, upward-coarsening units with beds that are laterally continuous for several kilometres. The upward-coarsening units are probably the product of individual regressive episodes and are interpreted as parasequences (*sensu* Van Wagoner *et al.*, 1990). These become sandier towards the north, indicating that the deposits become more proximal towards the north. It consists mainly of heterolithic, wavy to lenticularly bedded mudstones with up to 10 cm thick, mainly wave-rippled and sparsely current-rippled sandstone beds (Figs 8A, 11A, 11B and 15D). These heterolithic units contain sparse hummocky cross-stratified (Fig. 15E) and planar-parallel laminated sandstone beds up to 40 cm thick. The sandstone beds indicate strong wave activity and occasional storms (c.f. Dott & Bourgeois, 1982), whereas mud-rich heteroliths represent fair-weather deposition. Deposits of this facies association are therefore interpreted to have been deposited in a wave-dominated, tide-influenced embayment above storm-wave base but below fair-weather wave base, in the offshore transition zone. Unsorted beds with grain size ranging from fine sand to pebbles, containing shell fragments and extraformational clasts, also occur (Fig. 15F) and are interpreted as deposits of submarine debris flows. Dam & Surlyk (1998) observed granite boulders with diameters up to 1·5 m within such beds, which probably were sourced from gravelly highstand beaches at times of extreme storms or tsunamis.

Facies Association 9 – Shoreface

This facies association occurs as a single, *ca* 5 m thick laterally continuous sandbody only present in Areas D and E. This unit correlates to the base of the sharp-based distributary system of the Astartekløft Member to the north of these deposits (Fig. 4A). Facies Association 9 consists of fine-grained to medium-grained sandstone beds with wavy bedding, wave ripples, planar-parallel lamination, occasional cross-beds and large *Rosselia* burrows (Figs 8A, 11A, 11B and 15G). The succession is sharp-based and locally underlain by a pebble-rich horizon.

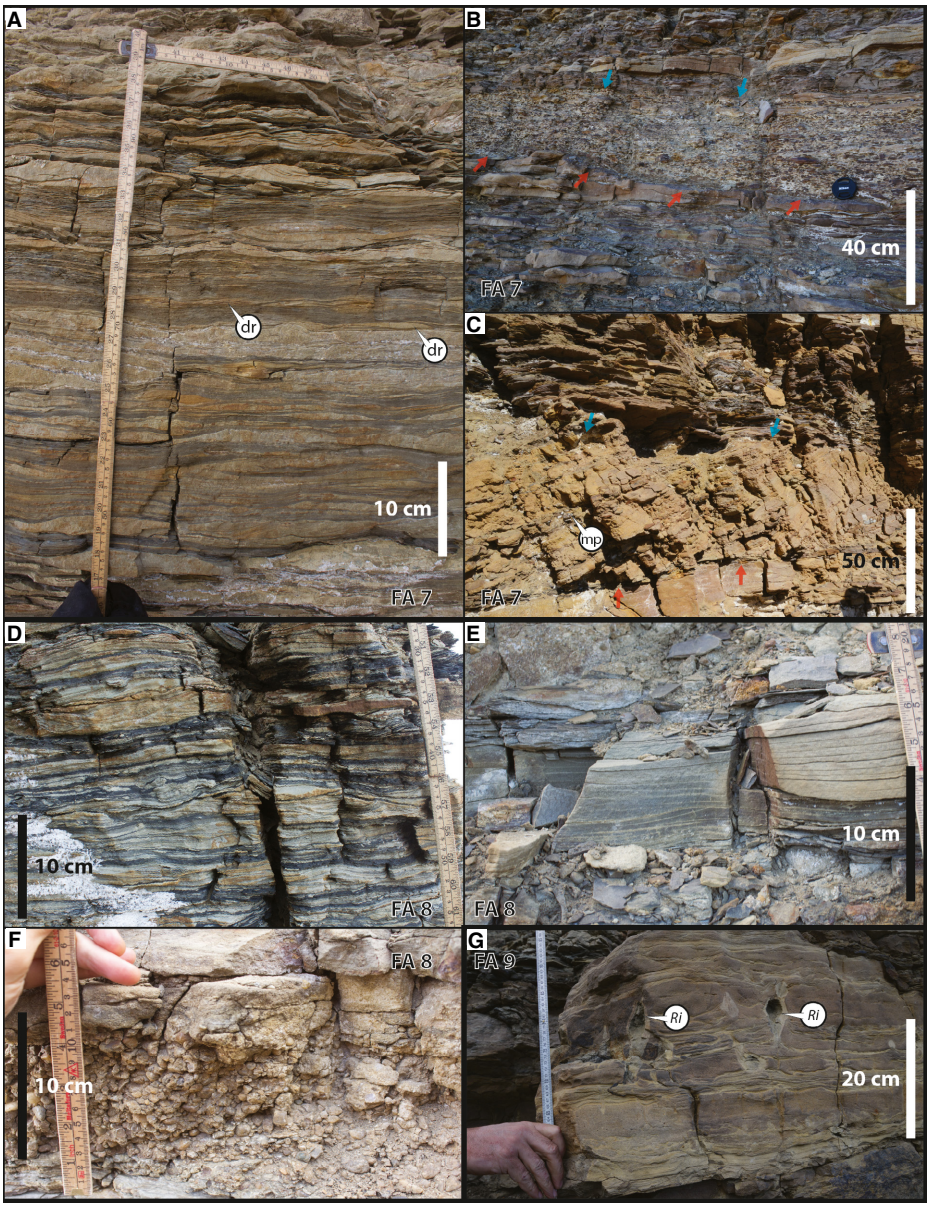

Fig. 15. Facies Associations 7, tidal flat (A) to (C); 8, offshore transition zone (D) to (F), and 9, shoreface (G). (A) Wavy-bedded, current-rippled and wave-modified current-rippled heteroliths typical for FA7. Current ripples are bidirectional, and transport direction is often opposite to the underlying layer. Occasional drowning ripples (dr) indicate high suspended load. From 51 m in log 3. (B) Erosively based, matrix-supported mud-pebble conglomerate underlain and overlain by wavy-bedded heteroliths. This facies occurs in 20 to 50 cm thick and 10 m wide, channel forms and is interpreted as deposits of tidal creeks. Base is marked by red arrows, top by blue arrows. From 69 m in log 1. (C) 50 cm thick deposit of inclined heterolithic stratification with mud pebbles (mp) and mudstone drapes on foresets, which occur rarely in FA7. Base is marked by red arrows, top by blue arrows. These are interpreted as the deposits of tidal creeks. From 78 m in log 1. (D) FA8: Mainly wave-rippled, wavy-bedded heteroliths of the Albuen Member consisting of siltstone and fine-grained sandstone. This facies makes up the majority of FA8. From 84 m in log 5. (E) FA8: Hummocky-cross-stratified fine-grained sandstone beds. These are occasionally observed in FA8, indicating a greater wave influence and water depth compared with the other facies associations. From 95 m in log 2. (F) 10 cm thick, clast-supported, rounded quartzitic pebbles in a matrix of medium-grained sandstone. Interpreted as a debris-flow deposit. From 87 m in log 3. (G) FA9: Poorly sorted, fine sandstone beds with *Rosselia* burrows (*Ri*). Wavy-bedded and faintly cross-bedded. Interpreted as a shoreface deposit. From 18 m in log 5.

The clean sandstone beds, dominance of wave-generated structures and the presence of marine bioturbation suggest a shoreface origin for these deposits (e.g. Clifton, 2006). The sharp base, locally underlying pebble horizon, small thickness compared with shorefaces described elsewhere (e.g. Hampson, 2010; Eide *et al.*, 2014) and direct correlations to a sharp-based channel system in the Astartekløft Member to the north suggest that this system may have been deposited during a forced regression (c.f. Plint, 1996).

DEPOSITIONAL ARCHITECTURE

Vertical and lateral relationship between facies associations

The different facies associations are arranged within consistent lateral and vertical trends (Fig. 16). Transgressive shoreface deposits (FA1) occur above the underlying Kap Stewart Group, and also as localized transgressive lags below the base of the FA8 deposits of the Albuen Member (Fig. 6). Facies Association 2 is interpreted as prodelta deposits and is gradationally overlain by FA3 (delta front). Facies Association 3 contains the unconfined tidal bar deposits of FA4 and is cut into by the distributary channels of FA6. Facies Association 4 lies laterally adjacent to the confined tidal bars of FA5 and above the delta-front deposits of FA3. Facies Association 5 is laterally adjacent to FA6 and the tidal-flat deposits of FA7. Facies Association 6 is always overlain by or contained within FA7. Furthermore, the wave-dominated offshore transition zone deposits of FA8 overlie the tide-dominated delta Facies Associations 3 to 7 in the entire study area.

Facies Associations 2 to 7 are genetically related as a progradational, tidally influenced delta system (Figs 9 and 16). Facies Associations 6 and 7 were deposited in large meandering channels and flanking tidal flats, and FA5 was deposited in the outermost tide-influenced distributary channels on the delta. These channels in turn supplied sediment to the delta front (FA3) and unconfined tidal bars (FA4). The most distal environment where sediment supply and energy was lowest is represented by the prodelta deposits of FA2.

Facies Association 8 overlies the delta platform facies associations (FA4 to FA7) over the entire study area, but thins and interfingers with FA7 towards the north. Facies Association 9 is only observed in the uppermost part of the study interval in Areas D and E and grades laterally into a sharp-based deposits similar to FA6 in Areas B and C (Fig. 4A). These sharp-based deposits lie unconformably on top of deposits of FA8. Facies Associations 1, 8 and 9 appear to occur predominantly or exclusively during transgressive episodes (Fig. 9).

Although the mean palaeocurrent directions are oriented normal to the studied outcrop (Fig. 5), the facies associations are consistently more proximal in the northern parts of the outcrop, compared to the south. Thus, even though the overall progradation direction was westward, it appears that the system prograded further in the northern areas.

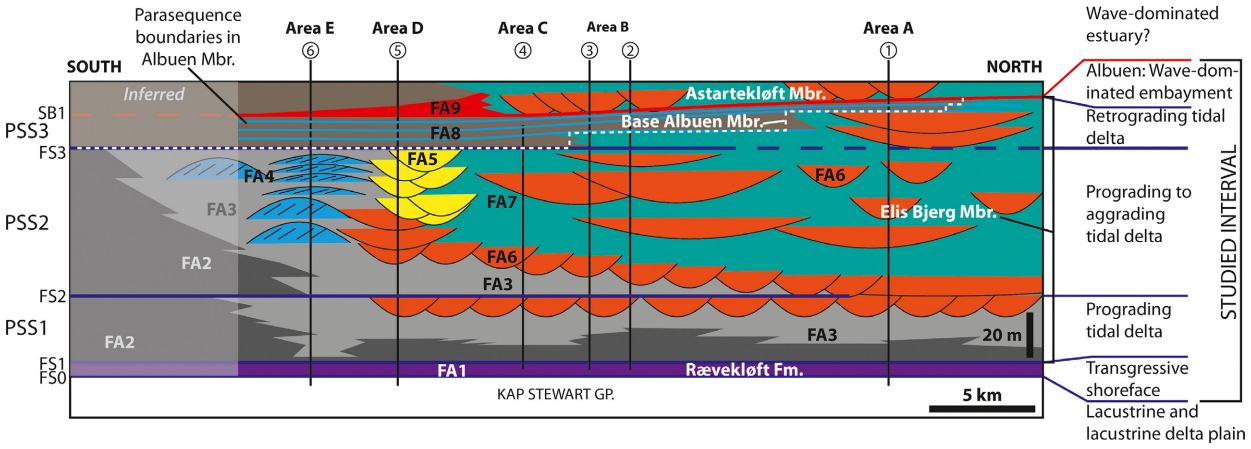

Fig. 16. Schematic cross-section oriented along depositional strike, showing the distribution of facies associations and stratigraphic surfaces in the studied interval.

Sequence stratigraphy

In shallow-marine and paralic settings, sequence stratigraphic models assume that changes in accommodation are driven by a combination of (tectonic and compaction-driven) subsidence and eustatic sea-level changes (e.g. Van Wagoner *et al.*, 1990; Helland-Hansen & Hampson, 2009). The aggradational to transgressive stacking pattern of parasequences observed in the Neill Klinter Group (Fig. 2) is interpreted as the result of an overall rise in relative sea-level (Surlyk *et al.*, 1973), probably related to post-rift thermal subsidence of the basin following a Triassic rift event (Surlyk, 2003) combined with eustatic sea-level rise in the early Jurassic (e.g. Haq *et al.*, 1987).

Parasequences

Tabular, upward-coarsening packages *ca* 4 to 8 m thick are common in the more distal facies associations in the study area: prodelta (FA2), delta front (FA3), unconfined tidal bars (FA4) and offshore transition zone (FA8) (Figs 4 and 11). In the southernmost part of the study area (Area E), these may be traced for more than a kilometre before they are covered by scree. The upward-coarsening packages are assumed to be deposited during gradual regression, and the sharp transitions to more mud-rich lower parts of overlying upward-coarsening packages are interpreted as abrupt deepening events. Thus, these are interpreted as parasequences (*sensu* Van Wagoner *et al.*, 1990), upward-coarsening units related to kilometre-scale landward displacement of the shoreline caused by alternating regressive periods and relative sea-level rises.

Although it was more challenging to define parasequences in the delta platform deposits (FA5 to FA7), laterally extensive and abrupt breaks in sandstone content have been correlated where possible (Fig. 6). Different facies belts (i.e. facies associations) are commonly not juxtaposed at the defined parasequence boundaries in more proximal areas, and it is generally not possible to demonstrate any landward displacement of the shoreline at parasequence boundaries in this study because it is a strike section.

The Albuen Member of the Gule Horn Formation shows well-defined upward-coarsening packages in FA8 that can be traced with confidence across the study area (Fig. 4). These deposits consist of four tabular parasequences (PS), termed PS N to PS Q (Figs 6 and 12E). The lowermost of these, PS N, grades northward into more sand-rich deposits of FA7 between Areas B and C. The second lowermost, PS O, grades into sandier deposits between Areas A and B. Facies belts are displaced at least 10 km northward at each of these parasequence boundaries. The outcrop is a strike section, and it is therefore not possible to accurately estimate the magnitude of shoreline displacement in the dip direction, but judging from the simple increase in sandstone from south to north and lack of evidence for an embayed coastline, it is likely that the coastline was displaced at least a few kilometres landward at each parasequence boundary.

Stratigraphic surfaces

Five stratigraphic surfaces, FS0 to FS3 and SB1, have been defined in the study area. These are defined where the sequence of facies associations cannot be explained by gradual progradation of facies belts alone, where a significant deepening spanning several facies belts occurs, or where a change in stacking pattern occurs. Four major flooding surfaces (FS0, FS1, FS2 and FS3) associated with a landward shift of facies belts, and one surface associated with a seaward shift of facies belts (sequence boundary, SB1), have been defined (Fig. 6).

The FS0 is defined at the lowermost occurrence of thick, poorly sorted sandstones with marine fossils (FA1), interpreted as transgressive shoreface deposits, on top of the underlying alluvial–lacustrine Kap Stewart Group (Fig. 6). This surface is planar across the entire facies belt. It is interpreted to represent a major transgressive surface associated with flooding and reworking of the underlying, low-lying lacustrine system of the Kap Stewart Group.

The FS1 is defined where the poorly sorted sandstones of FA1 are overlain by mudstone-rich, rippled heteroliths of FA2, interpreted as prodelta deposits. This surface is planar over the entire study area (Figs 4 and 6). The decrease in energy from FA1 to FA2, together with the upward-coarsening motif observed above the FS1, indicates that this surface is associated with further flooding, displacing the shoreline landward from the outcrop belt and leading to relatively deep marine waters with low wave energy in the study area.

The FS2 is associated with distributary channel (FA6a) and coarse-grained delta-front (FA3) deposits being overlain by mudstone-rich delta-front deposits (FA3) in Areas C, D, E and probably B of the study area (Fig. 6). This surface cannot be correlated to a facies belt dislocation

in Area A, but may correlate to the top of a channel body which occurs at the appropriate stratigraphic level in this area. This surface is interpreted to represent a minor flooding event displacing the shoreline system in the southern parts of the study area only.

The FS3 is picked at the first occurrence of FA8 (offshore transition zone deposits) in the outcrop belt (Fig. 6) and correlated northward from here. It is obvious from the virtual outcrops that the base of FA8 in Areas C to E does not correlate to the base of FA8 further north, but rather to reworked surfaces within the tidal-flat deposits (FA7) in log 3. This shows that the base of FA8 is not a facies shift over the entire study area, but rather marks the transition from progradational/aggradational to retrogradational stacking of parasequences. In Area A, the FS3 is tentatively correlated to the base of a set of very wide channels (Figs 4E and 6), because this marks a pronounced change at the expected stratigraphic level of FS3. This is discussed further below.

The SB1 is placed where erosively based cross-stratified sandstone beds (FA6a, Fig. 4A), sharp-based tidal-flat deposits (FA7) and sharp-based shoreface deposits (FA9) unconformably overlie the mudstone-rich offshore transition deposits (FA8) of the Albuen Member (Fig. 6). This surface is relatively planar without any obvious scours (Figs 4 and 6) and corresponds to the base of the Astartekløft Member of the Ostreaelv Formation. North of the study area, the Albuen Member is completely eroded at this boundary (Fig. 2; Ahokas *et al.*, 2014a). It follows from the facies relationships (distributary channels on top of offshore transition zone deposits) that a large amount of erosion and truncation of facies belts occurred at the SB1 in the northern part of the study area and that the erosion decreased southward to Areas D and E (sharp-based shoreface deposits onto offshore transition zone deposits).

Parasequence sets

The studied deposits of the Gule Horn Formation have been divided into three parasequence sets (PSS1 to PSS3; Figs 6 and 16), based on stacking patterns of facies associations and parasequences, and the four major flooding

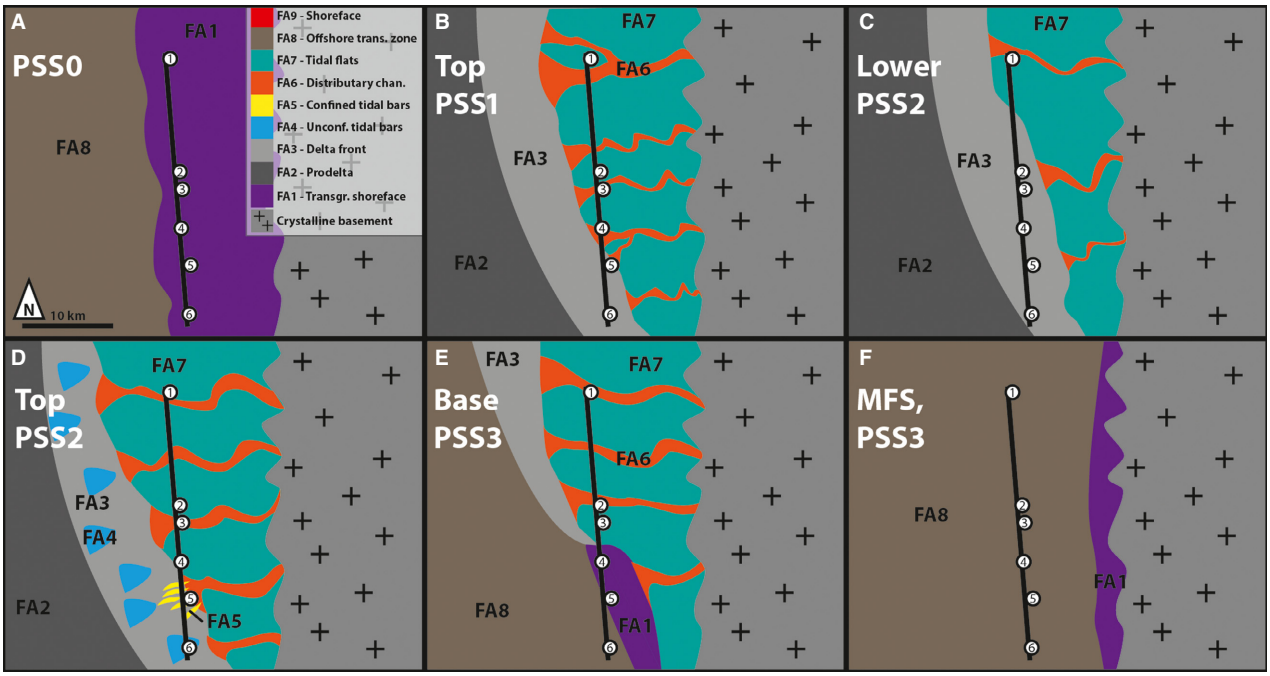

Fig. 17. Palaeogeographic maps showing plan-view distribution of facies associations in the studied deposits at selected time intervals. (A) Deposition of the Rævekløft Formation during the transgression of the Kap Stewart Group. (B) Maximum transgression during parasequence set 1 (PSS1). (C) Base of PSS2 immediately after the transgression of PSS1. Note that there is no noticeable landward displacement of facies belts in the northern part of the study area. (D) PSS2 at maximum regression of the Elis Bjerg Member. (E) Base of PSS3. The southern part of the study area is transgressed, while FA6 and FA7 are still being deposited in the northern part. (F) Maximum flooding at the base of PS Q led to the transgression of the shallow-marine system in the entire study area.

surfaces: FS0 marks the flooding of the underlying Kap Stewart Group, FS1 marks the flooding of the Rævekløft Formation, FS2 is a flooding event within the Elis Bjerg Member and FS2 marks the base of the Albuen Member in the southern part of the study area (Areas C to E) and the onset of retrogradational parasequence stacking in the rest of the study area. The plan-view distribution of facies associations during the evolution of the system is illustrated in Fig. 17.

Rævekløft Formation

The Gule Horn Formation is a tabular deposit of FA1, which has been interpreted as a shoreface deposited as the underlying alluvial–lacustrine Kap Stewart was transgressed (Dam & Surlyk, 1998). The base and top of this unit are major flooding surfaces (FS0 and FS1).

In the southernmost part of the outcrop (log 6, Fig. 6), two stacked 9 m thick sandstone bodies separated by a 1·2 m thick, more siltstone-rich interval of FA2 (prodelta) occur. Both of these bodies were assigned to the Rævekløft Formation by Dam & Surlyk (1998), but the facies and stratigraphic thickness indicates that the upper package is more likely to correlate to the lower part of the Gule Horn Formation.

Parasequence set 1

The PSS1 is bounded below by FS1 and above by FS2 (Fig. 6). In Areas A to D, this parasequence set records a shallowing-upward succession, from prodelta (FA2) via delta front (FA3) to distributary channels (FA6). The distributary channels are erosively based, but the lower boundary is relatively planar over the study area, without any outsize scours (c.f. Willis & Gabel, 2003). This suggests that they were deposited during normal regression of facies belts, and no evidence for a significant relative sea-level fall at this level, as interpreted by Dam & Surlyk (1998, SB3), has been observed. In the southernmost part of the study area (log 6, Fig. 6), PSS1 consists of three upward-coarsening parasequences consisting of FA2 (prodelta) and FA3 (delta front) deposits; FS2 is placed at the top of the most coarse-grained deposits in log 6, planar heteroliths consisting of wavy-bedded siltstone and poorly sorted medium-grained sandstone containing abundant extraformational pebbles.

Parasequence set 2

The PSS2 is bounded below by FS2 and above by FS3. In the northernmost and most proximal area (Area A, Fig. 4e), FS2 is not associated with a dislocation of facies belts, but is rather placed on top of a channel body. In logs 2 to 5, PSS2 comprises delta-front (FA3) deposits in the lowermost part, which coarsen upward and are overlain by erosively based deposits of FA6 (distributary channels). Areas B and C record transitions between distributary channels (FA6) and tidal flats (FA7) for the upper part of PSS2, while more distal confined tidal bars (FA5) occur in Area D (Fig. 4C). In Area E, PSS2 mostly consists of delta-front (FA3) deposits in the lower part and unconfined tidal bars (FA4) in the upper part. Thus, this parasequence set records a progradational to aggradational facies pattern in the southern parts of the area (Areas B to E; Figs 4A and 6) and an aggradational pattern throughout in the northernmost part (Area A).

Parasequence set 3 (Albuen Member and parts of the Elis Bjerg Member in the north)

The PSS3 is bounded below by FS3, which marks the base of offshore transition zone deposits (FA8) in Areas C and D, and above by the sharp-based sandstones of the Astartekløft Member of the Ostreaelv Formation (Fig. 6). The lowermost parasequence in PSS3 becomes more sand-rich towards the north and grades into tidal flats (FA7) in Area B (Fig. 6). The following parasequence, PS O also coarsens towards the north, and consists of FA8 in Area B. Long-range correlations over the 12 km long, scree-covered area between Areas A and B, suggest that PS O correlates to FA6 (distributary channel) and FA7 (tidal flat) in Area A. The two uppermost parasequences consist of offshore deposits over the entire area, indicating that the delta was fully transgressed in the study area at this interval. The maximum flooding surface within the Gule Horn Formation is placed at the base of PS Q, because this is the most fine-grained interval in PSS3. The base of the Albuen Member in the southern part of the study area defines a retrogradationally stacked parasequence set, representing gradual flooding and backstepping of the Elis Bjerg delta, where the areas in the northern part of the study area (Area A) with greatest sediment supply were flooded last. This explains the northward thinning of the Albuen Member.

Summary

In summary (Figs 17 and 18), the Rævekløft Formation is the result of a rapid, large-scale trans-

gression of the lacustrine Kap Stewart Group. The FS0 represents erosion as the marine shorelines encroached over the Kap Stewart Group, and the FS1 formed due to further deepening of the basin. The PSS1 represents a first progradational pulse of a tide-dominated delta, which was transgressed in the southern part at FS2. In the northern part of the study area, sediment supply was large enough to keep up with accommodation creation in the basin, and no facies belt dislocation occurred. Following the FS2, the PSS2 prograded and then aggraded, with more proximal facies associations developed in the north than in the south. In PSS3, the system is retrogradationally stacked, and each parasequence records a more landward position of FA8, reflecting flooding of the tidal delta system progressively towards the north. Because the base of the Albuen Member is defined as the base of the offshore heteroliths of FA8, this is an example of a lithostratigraphic boundary not coinciding with a sequence stratigraphic boundary (c.f. Bhattacharya, 2011). The two uppermost parasequences in PSS3, which overlie the maximum flooding surface, are highstand deposits with shorelines located landward of the outcrop belt. The debrites in FA8 are observed to contain rounded, extraformational pebbles which indicate that the highstand shorelines were pebbly beaches. Greater wave influence in the distal parts of PSS3 compared to the deposits of PSS1 and PSS2 is indicated by the presence of more well-developed wave ripples and the presence of hummocky cross-stratification. This might indicate a larger basin and reduced tidal influence. The juxtaposition of the distributary channels (FA6) of the Astartekløft Member on top of the wave-dominated embayment (FA8) is the only facies contact in the studied succession that requires a fall in relative sea-level and major forced regression of facies belts.

DISCUSSION

Comparison with previous work in the area

Application of helicopter-based LiDAR scanning and generation of virtual outcrops have made it possible to trace beds over large distances, to make improved correlations and to define internal architecture in sedimentary bodies. The facies associations defined in this study broadly agree with the interpretations of Ahokas *et al.* (2014a, b), but are on a finer scale. Table 3 shows how the facies associations used in this study fit into the architectural elements of Ahokas *et al.* (2014a). Some subtle changes to the existing sequence stratigraphic framework (Dam & Surlyk, 1998; Ahokas *et al.*, 2014a) are suggested (Table 4).

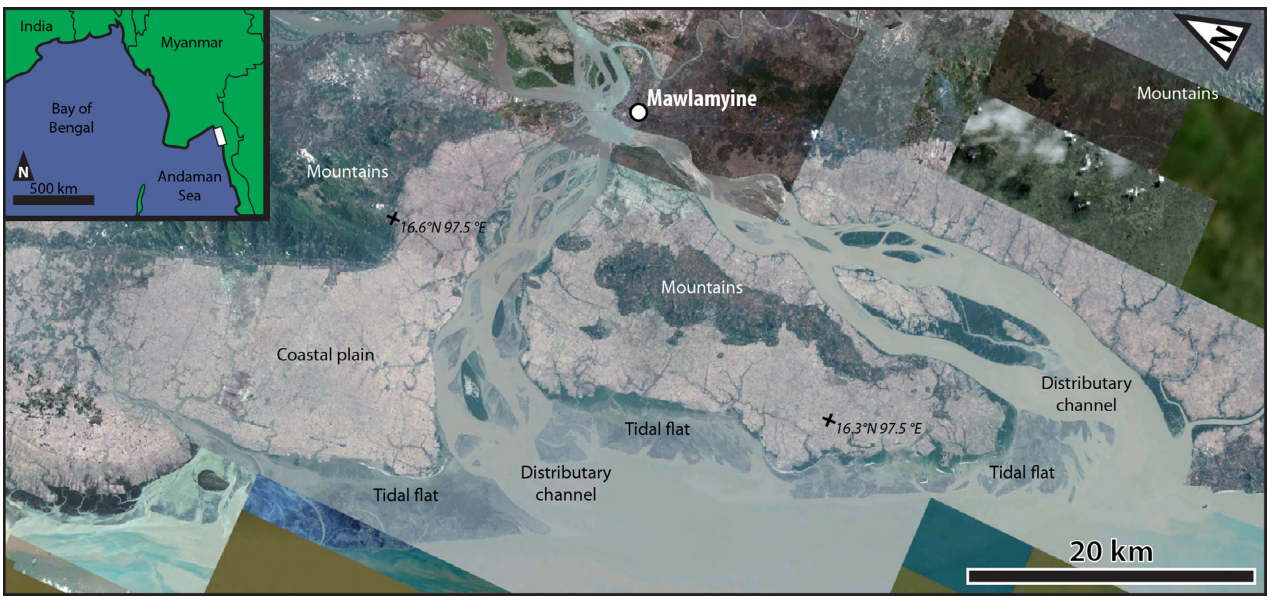

Fig. 18. A suggested modern analogue for the Elis Bjerg delta: the Salween River delta, near Mawlamyine, Mon State, Myanmar. See inset map for location. The Salween River delta exhibits extensive tidal flats and kilometre-wide distributary channels with prograding tidal bars. It has a narrow coastal plain which onlaps the nearby mountains. Image data © Google 2013.

Table 3. Comparison between facies associations used in this study and relevant architectural elements used by Ahokas *et al.* (2014a). The architectural elements are broader environments which several of the facies associations defined in this study fit into. Note that the inshore tidal facies associations (FA5 to FA7) can exist in both the TDDP and TDSS (regressive and transgressive, respectively) architectural elements.

Architectural element (Ahokas *et al.*, 2014a)		Facies association (this study)		Subordinate architectural elements
Code	Name	Code	Name	Code
TDSS	Tide-dominated subtidal sandy shoal	FA9	Shoreface	–
WDBE	Wave-dominated brackish-marine embayment	FA8	Offshore transition zone	–
TDDP	Tide-dominated/influenced delta platform	FA7	Tidal flat	TDSS
		FA6	Distributary channels	TDSS
		FA5	Confined tidal bars	–
TDDF/ TDDP	Transitional between TDDF and TDDP	FA4	Unconfined tidal bars	–
TFFD	Tide-dominated delta front	FA3	Delta front	–
		FA2	Prodelta	–
SHFS	Shoreface–foreshore sandstone	FA1	Transgressive shoreface	TDSS

The base of distributary channels in PSS1 ('within-trend normal regressive surface' in Fig. 6) was interpreted as a sequence boundary by Dam & Surlyk (1998). In the present study, this surface is rather interpreted as having formed as wide or widely meandering distributary channels prograded onto the delta front. Ahokas *et al.* (2014a) interpreted the overlying surface, termed FS2 in this study, as a facies transition from distributary channels to tidal flats. This surface is rather interpreted as a major flooding surface, leading to deposition of delta-front deposits (Fig. 6), based on the regional extent of the surface and lack of channelized erosion features commonly observed in tidal-flat environments.

The base of the Astartekløft Member, SB1 was interpreted as a coalesced subaerial unconformity and transgressive surface along its entire length by Ahokas *et al.* (2014a,b). This surface is planar but erosive in the study area for the present article and completely erodes away the Albuen Member north of the study area (Fig. 2). It is underlain by wave-dominated heteroliths of FA8 and overlain by cross-bedded sandstones with mudstone drapes and tidal bundling in the northern part of the study area (Areas A to C, Figs 4 and 6), interpreted as the deposits of tide-influenced distributary channels. However, in the southern part of the outcrop, which was not studied by Ahokas *et al.* (2014a,b), this surface correlates with a sharp-based shoreface deposit (FA9; logs 5 and 6, Fig. 6), interpreted as a shoreface sandbody *within* the Albuen Member by Dam & Surlyk (1998). This interpretation is not supported by the analysis performed on the virtual outcrop dataset. It is suggested that the first occurrence of FA9 in the southern parts of the study area correlates to SB1.

The offshore transition deposits (FA8) of the Albuen Member underlying SB1 show an upward-coarsening trend (log 5, Fig. 6), which indicates progradation just underneath this surface. The SB1 is, therefore, interpreted to have formed as a result of forced regression of the highstand shorelines of the Albuen Member, leading to the deposition of nearshore deposits in the southern part of the study area. The base of the Astartekløft Member is therefore an 'attached lowstand' (*sensu* Ainsworth & Pattison, 1994). North of the study area, offshore transition deposits (FA8) at the Albuen Member interval are absent (Fig. 2), and the SB1 shows a greater magnitude of erosion (Ahokas *et al.*, 2014a,b). Thus, the SB1 is a coalesced *transgressive surface* and *subaerial unconformity* (SB1) north of Harris Fjeld, a *subaerial unconformity* developed at the base of forced regressive distributary channels in Areas A to C, and

Table 4. Comparison between important sequence stratigraphic surfaces and their significance in this study and Ahokas *et al.* (2014a).

This study		Ahokas *et al.* (2014a)		
Code	Significance	Code	Significance	Difference
SB1	Forced regression of shorelines to the Albuen Area	SU1/TS3	Coalesced sequence boundary and transgressive surface over the study area	Interpreted in this paper as a regressive facies shift, representing forced regression of environments in the study area
MFS	Maximum flooding of the study area during deposition of the Gule Horn Formation	MFS2	Maximum flooding of the study area during the Gule Horn Formation	None
FS3	Flooding of the Elis Bjerg shorelines in the southern parts of the study area (Areas C to E), onset of retrogradational parasequence stacking pattern over the entire study area	TS2	Flooding of the Elis Bjerg Member shallow-marine system	Coincides in the southern part (Areas C to E), but TS2 of Ahokas *et al.* (2014a) north of Albuen is in this paper considered a diachronous facies boundary (Figs 16 and 18)
FS2	Kilometre-scale landward displacement of the Elis Bjerg Member shorelines in southern parts of the study area	FSb	Minor flooding surface within the Elis Bjerg Member	Greater magnitude of landward displacement of shorelines interpreted in this study
FS1	Flooding and abandonment of the wave-dominated transgressive shoreface of the Rævekløft Formation	FSa	Flooding and abandonment of the wave-dominated transgressive shoreface of the Rævekløft Formation	None
FS0	Flooding of the alluvial–lacustrine environments of the Kap Stewart Group	TS1	Flooding of the alluvial–lacustrine environments of the Kap Stewart Group	None

a *regressive surface of marine erosion* in Areas D and E. Detached lowstand deposits are, therefore, not predicted further seaward. Furthermore, a significantly increased abundance of extraformational clasts at the base of the SB1, as noted by Ahokas *et al.* (2014a,b), has not been observed in this study. Extraformational pebbles appear to be present at the base of most channelized facies associations in the area (Fig. 6), and it does not seem justified to use this criterion to argue for subaerial exposure and erosion in the study area in the Jameson Land Basin.

Estimation of net shoreline trajectory of parasequence sets

The Elis Bjerg Member has a dominance of seaward-directed palaeocurrents throughout, and seaward-directed forward accretion surfaces in the unconfined tidal bars (FA4, Fig. 15). The average grain size decreases palaeoseaward (Fig. 6). The Elis Bjerg Member is generally without marine body fossils, but contains relatively abundant terrestrial-derived material, such as logs and plant fragments. This indicates a dominance of seaward-directed sediment transport. It is underlain by a major flooding surface (FS1) and prodelta deposits (FA2) that coarsen upward towards an erosion surface interpreted as the base of extensive distributary channels (FA6), which indicates progradation of the system. The Elis Bjerg Member contains two laterally extensive incision surfaces (Fig. 16), but these are not associated with significant seaward facies shifts, but rather represent the gradual progradation of erosively based distributary channels over the delta front. The system shows

an overall progradational stacking pattern in PSS1 and PSS2, only briefly interrupted by a minor flooding at the FS2 in the southern part of the study area (Fig. 6). Based on these criteria, the parasequence sets PSS1 and PSS2 of the Elis Bjerg Member are interpreted as the deposits of an overall prograding shoreline system (i.e. a delta).

The PSS3, which consists of the lithostratigraphically defined Albuen Member and upper parts of the Elis Bjerg Member in the north (Figs 2 and 6), is retrogradationally stacked, although the individual parasequences are upward coarsening. This indicates that this part of the Elis Bjerg is retrogradational, and is therefore a net retrogradational shallow-marine system, and an estuary by definition (Dalrymple & Choi, 2007).

An estuary is a system fed by both marine and fluvial processes and would, therefore, have a bedload convergence zone, recording a balance between seaward and landward sediment transport, and commonly has a grain-size minimum in the centre of the system (Dalrymple *et al.*, 1992; Dalrymple & Choi, 2007). Estuaries are transgressive environments and would be underlain by an erosion surface and record more distal facies succession upward (Dalrymple *et al.*, 1992). The overlying Astartekløft Member is underlain by an erosion surface which juxtaposes distributary channels on top of shelfal deposits (Fig. 6) and is therefore interpreted as an estuary (c.f. Ahokas *et al.*, 2014b). However, it is important to note that these units are estuaries in the sense that they are retrogradational tide-influenced shallow-marine systems (Dalrymple & Choi, 2007) and not in the classical sense of a terraced, drowned palaeovalley (e.g. Dalrymple *et al.*, 1992). The latter type of estuary is also present in the Neill Klinter Group, but only north of the study area (Ahokas *et al.*, 2014b).

Palaeogeographic implications

The immaturity of the sediments indicates short transport distances and an irregular topography in the source area. Provenance studies show that the sediments in the Neill Klinter Group (Fig. 2) were sourced from the crystalline basement in nearby Liverpool Land (Slama *et al.*, 2011), which is onlapped by Mesozoic strata (Ahokas *et al.*, 2014a; Fig. 1). Liverpool Land is mountainous today, and the immature sedimentary textures in the study area indicate that it also had a significant topography at the time of deposition of the Gule Horn Formation. It is likely that the distance from the sediment source area in Liverpool Land to the studied outcrop belt was the same as it is today (Fig. 1). The short inferred distance from the sediment source combined with the parallel palaeocurrent directions suggests a line-sourced system rather than a radial fan. However, it is likely that an input point near Harris Fjeld in the northern part of the study area supplied more sediment than the others, due to the consistently more proximal facies associations, greater proportion of sand and coarser grains in the northern part of the study area. Liverpool Land today is small with minor watersheds and is probably too small to have supplied a delta system of the magnitude that is described for the Elis Bjerg Member. However, Liverpool Land was attached to a much larger land mass until the separation of the Jan Mayen Microcontinent from East Greenland in the latest Eocene (e.g. Lundin & Doré, 2002; Mjelde *et al.*, 2008; Fig. 1), which gives a potential for larger catchments during this time.

In log 1, the thickness of the Gule Horn Formation is 115 m, while it is on average 98 m in the other logs (95 to 103 m). This probably indicates greater subsidence in the northern part, possibly due to increased loading because of larger sediment supply or somewhat larger post-depositional compaction in the more mudstone-rich sediments in logs 2 to 6 (Fig. 6). Together with the more distal facies in the southern part, this indicates a higher sediment supply in the northern parts of the study area. This pattern is observed in the entire Neill Klinter Group (for example, the Harris Fjeld Member of the Ostreaelv Formation, Fig. 2) and implies a long-lived, structurally controlled sediment entry point around Harris Fjeld.

Significance of the lack of subaerial deposits

No evidence of subaerial exposure, such as the presence of coal beds, desiccation cracks or rooted horizons, is observed within the studied interval. Possible interpretations for the absence of supratidal or coastal plain facies are: (i) that the delta built out mostly subaqueously and had a restricted coastal plain which never prograded to the study area; (ii) removal of coastal plain deposits by widely meandering tidal channels; (iii) removal of coastal plain by transgressive erosion at parasequence boundaries; or (iv) that the delta had wide subtidal and intertidal flats and a

restricted coastal plain that never prograded to the outcrop belt. Täanavsuu-Milkeviciene & Plink-Björklund (2009) discussed differences between tide-dominated versus tide-influenced deltas, most notably that tide-influenced deltas normally develop coastal plains, while tide-dominated deltas are overlain by extensive subaqueous tidal flats. For example, the modern, tide-dominated Changjiang delta (Hori *et al.*, 2002) shows an approximately 50 km wide subaqueous delta platform consisting of mainly subtidal sandflats between the coastline and the delta front. This is probably not a good analogue for the system in the Elis Bjerg Member, because of the obvious channels present in FA5, FA6 and FA7 (Figs 14 and 15A to C). It seems unlikely that channels with well-defined, relatively steep cut banks with evidence for cut-bank failure (FA5) and inclined heterolithic stratification (FA7) could develop fully subaqueously.

It is possible that subaerial deposits were removed by transgressive erosion at parasequence boundaries (c.f. Willis *et al.*, 1999; Hwang & Heller, 2002) or by regressive erosion at the base of distributary channels and tidal bars (c.f. Pontén & Plink-Björklund, 2009). However, it is regarded as less likely that these processes could have removed subaerial deposits to such a complete degree over the entire study area. It is, therefore, suggested that the proximal parts of the studied deposits developed as extensive subtidal to intertidal flats (FA7), drained by numerous minor tidal creeks and cut by widely meandering distributary channels which were filled by tidal dunes and bars (FA6), and that supratidal deposits were developed further landward.

Process regime

The sparse wave-generated structures suggest that the Elis Bjerg system was not deposited on an open coast. This is consistent with regional palaeogeographical studies, which placed the Early Jurassic of the Jameson Land Basin in a structurally controlled embayment connected to a narrow, tide-influenced seaway (e.g. Dam & Surlyk, 1998; Surlyk, 2003; Fig. 1).

Most facies in the studied deposits contain some indication of tidal influence. The heterolithic facies contain bidirectional current ripples or high-frequency sand–mud alterations. Sandstone beds contain abundant mudstone drapes on cross-bed foresets, and other features caused by slack-water periods and flow reversal associated with tides, such as cyclical bundle thickness variations, and oppositely directed cross-beds ('herringbone cross-stratification') are also observed. However, the majority of palaeocurrent readings from cross-bed foresets record palaeoseaward (westward) transport (Fig. 5) and no evidence of mutually evasive tidal channels are observed. The dominance of ebb-oriented palaeocurrents, overall progradational motif, abundant terrestrial-derived organic fragments and lack of marine body fossils, indicates a strong fluvial influence. The more fine-grained facies associations (FA2, FA3, FA7 and FA8) contain abundant wave ripples, but hummocky cross-stratification is only observed sporadically in the Albuen Member. Shoreface deposits are present only in the underlying Rævekløft Formation and the overlying Astartekløft Member of the Ostreaelv Formation (Fig. 2). Thus, the deposits are influenced by tides, river currents and waves. The imprint of waves is relatively minor within the regressive Elis Bjerg Member, but is higher in the transgressive Rævekløft Formation (PSS0) and net transgressive Albuen Member (distal parts of PSS3). Applying the classification scheme of Ainsworth *et al.* (2011) and Vakarelov & Ainsworth (2013), the studied deposits belong to the Tf*w*-category (tide-dominated, fluvial-influenced and wave-affected).

A modern analogue for this system must include extensive tidal flats, wide distributary channels, a near-absence of wave-dominated elements, a parallel distributary pattern and close proximity to the sediment source. The Salween River delta of Myanmar (Fig. 18) satisfies these criteria and demonstrates that the model proposed in this study is possible.

Nature of channels

The distributary channels (FA6) in this study are erosively based, upward fining 3 to 12 m thick sheets wider than a few kilometres, which occasionally contain low-angle dipping surfaces, interpreted as lateral accretion surfaces. Channel beds have a relief of less than 0·5 m. Distributary channels in modern tide-dominated systems are between 5 m and 15 m deep (Willis, 2005), and the observed channels in the Elis Bjerg Member fit well within these observations. There are no deep erosion surfaces indicating either extreme deepening of channels due to tidal scouring, as observed in many ancient and modern systems (Willis & Gabel, 2003; Choi *et al.*, 2004) or incised valleys (e.g. Ahokas

et al., 2014b). The observed channel belts were very wide compared with what has been observed in other studies, suggesting that the channels are wide or widely meandering. This could be caused by increased erodibility of the banks due to coarser grain size and lack of vegetation in the study area.

Distributary channel bodies of FA6 appear to be narrower in the upper half of parasequence set 2 (PSS2) in the northern part of the study area than anywhere else (Area A, Figs 4E and 16). This is interpreted to be the most proximal part of the deposits and indicates that the tide-influenced distributary channels observed in this study become wider closer to the shoreline. This observation is consistent with current models of deposition in tide-dominated depositional systems, which predict funnel-shaped and seaward-flaring channels (Dalrymple & Choi, 2007; Vakarelov & Ainsworth, 2013).

CONCLUSIONS

Nine facies associations have been defined in the Rævekløft and Gule Horn formations in Jameson Land, Eastern Greenland, on the basis of lithological expression in logs and appearance in outcrops. The studied deposits contain poorly sorted, coarse-grained sediments and abundant terrestrial-derived wood fragments, record predominantly seaward-directed palaeocurrents, and contain abundant evidence for tides. The studied succession is interpreted as the deposits of a prograding and later retrograding tide-dominated delta with strong river-influence and weak wave-influence. Wave-processes appear to be more pronounced during transgressive periods. The tide-dominated delta is interpreted to lie close to uplands with significant topography because of the immaturity of the sedimentary rocks and regional stratal relationships.

In coarse-grained, tide-dominated delta systems, lithological variation on a facies scale can be bewildering, with great variation in grain size and sedimentary structures over short vertical distances. However, the large-scale architecture of the Gule Horn Formation shows relatively simple lateral variations, dominated by wide facies belts and wide channels. Sandy channel bodies become narrower in more proximal areas, consistent with seaward-flaring channels often observed in modern tidal systems. The great width of facies belts is probably related to a large tidal range and low-lying sedimentary nature of the landscape, which distributes similar environmental conditions over a large area. This leads to greater distance from the delta front to subaerial coastal plain deposits compared with other delta types. In contrast to dominantly fine-grained tidal deltas where channels are mainly filled by well-defined inclined heteroliths, channels in coarse-grained tidal deltas are rather filled by amalgamated sandy tidal dunes and bars consisting of cleaner, pebbly sandstone.

The Gule Horn Formation has been divided into three, mostly tabular parasequence sets (PSS). The PSS1 is progradational and records the progradation of a tide-dominated delta, spanning prodelta, delta-front and distributary channels. The overlying parasequence set (PSS2) occurs above this major flooding surface and records progradation and later aggradation of the system. The upper part of PSS2 is characterized by a proximal–distal facies succession from wide distributary channels flanked by extensive tidal flats in the north of the study area, confined tidal bars in the medial part and forward-aggrading unconfined tidal bars in the distal parts. The PSS2 is overlain by the retrogradationally stacked PSS3, in which wave-dominated offshore transition zone heteroliths overlie the tide-dominated delta. Successive parasequences in the PSS3 record a progressive flooding of the delta system from south to north, until the tide-dominated delta system is fully transgressed in the study area. Finally, sharp-based distributary channels and shoreface deposits overlying the PSS3 indicate a relative sea-level fall at the base of the attached lowstand deposits of the Astartekløft Formation.

The most proximal areas in the Elis Bjerg Formation show extensive subtidal to lower intertidal flats dissected by tidal creeks interspersed with kilometres wide tide-influenced distributary channels, which are filled by sandy tidal dunes and tidal bars. Medial parts of the studied deposits occur as upward coarsening, channelized tidal bars with abundant fluid muds at the bases, which is characteristic of confined, elongate tidal bars which occur near the turbidity maximum on the outer parts of tide-dominated deltas. These grade into sandy unconfined, downcurrent-stepping tidal bars, which contain pronounced clinoforms; these are probably analogous to mouth bars in river-dominated deltas. In the most distal reaches, heterolithic, planar delta front and muddy prodelta deposits occur.

ACKNOWLEDGEMENTS

Funding for this project was provided from the Research Council of Norway through the Petromaks project 193059 and the FORCE Safari Project. Arild Andresen (University of Oslo) and Aka Lynge (POLOG) are thanked for logistical support, Björn Nyberg (Uni Research CIPR and University of Bergen) for assistance in the field, Arve Næss (Statoil) for providing data and assistance during the planning phase, Julien Vallet and Huges Fournier (Helimap Systems SA) for data acquisition. Riegl LMS GmbH is acknowledged for software support. We thank Brian Willis and an anonymous reviewer for their insightful and thorough reviews and Mariano Marzo for editorial comments.

REFERENCES

Ahokas, J.M., **Nystuen, J.P.** and **Martinius, A.W.** (2014a) Depositional dynamics and sequence development of the paralic Early Jurassic Neill Klinter Group, Jameson Land Basin, East Greenland: comparison with the Halten Terrace, mid-Norwegian continental shelf. In: *From Depositional Systems to Sedimentary Successions on the Norwegian Continental Shelf* (Eds A.W. Martinius, R. Ravnås, J.A. Howell, R.J. Steel and J.P. Wonham), *Int. Assoc. Sedimentol. Spec. Publ.*, **46**, 291–333.

Ahokas, J.M., **Nystuen, J.P.** and **Martinius, A.W.** (2014b) Stratigraphic signatures of punctuated rise in relative sea-level in an estuary-dominated heterolithic succession: incised valley fills of the Toarcian Ostreaelv Formation, Neill Klinter Group (Jameson Land, East Greenland). *Mar. Petrol. Geol.*, **50**, 103–129.

Ainsworth, R.B. and **Pattison, S.A.J.** (1994) Where have all the lowstands gone? Evidence for attached lowstand systems tracts in the Western Interior of North America. *Geology*, **22**, 415–418.

Ainsworth, R.B., **Vakarelov, B.K.** and **Nanson, R.A.** (2011) Dynamic spatial and temporal prediction of changes in depositional processes on clastic shorelines: toward improved subsurface uncertainty reduction and management. *AAPG Bull.*, **95**, 267–269.

Ashley, G.M. (1990) Classification of large-scale subaqueous bedforms; a new look at an old problem. *J. Sed. Petrol.*, **60**, 160–172.

Baas, J.H. (2000) EZ-ROSE: a computer program for equal-area circular histograms and statistical analysis of two-dimensional vectorial data. *Comput. Geosci.*, **26**, 153–166.

Bhattacharya, J.P. (2011) Practical problems in the application of the sequence stratigraphic method and key surfaces: integrating observations from ancient fluvial-deltaic wedges with Quaternary and modelling studies. *Sedimentology*, **58**, 120–169.

Brandsæter, I., **McIlroy, D.**, **Lia, O.**, **Ringrose, P.** and **Næss, A.** (2005) Reservoir modelling and simulation of Lajas Formation outcrops (Argentina) to constrain tidal reservoirs of the Halten Terrace (Norway). *Petrol. Geosci.*, **11**, 37–46.

Buckley, S.J., **Vallet, J.**, **Braathen, A.** and **Wheeler, W.** (2008a) Oblique helicopter-based laser scanning for digital terrain modelling and visualization of geological outcrops. *Int. Arch. Photogrammetry Remote Sens. Spatial Inform. Sci.*, **37**, 493–498.

Choi, K.S., **Dalrymple, R.W.**, **Chun, S.S.** and **Kim, S.P.** (2004) Sedimentology of modern, inclined heterolithic stratification (IHS) in the macrotidal Han River delta, Korea. *J. Sed. Res.*, **74**, 677–689.

Clifton, H.E. (2006) A Reexamination of facies models for clastic shorelines. In: *Facies Models Revisited* (Eds H.W. Posamentier and R.G. Walker), *SEPM Spec. Publ.*, **24**, 126–184.

Dalland, A., **Worsley, D.** and **Ofstad, K.** (1988) A lithostratigraphic scheme for the Mesozoic and Cenozoic succession offshore mid- and northern Norway. *Norw. Petrol. Direct. Bull.*, **4**, 1–65.

Dalrymple, R.W. and **Choi, K.** (2007) Morphologic and facies trends through the fluvial-marine transition in tide-dominated depositional systems: a schematic framework for environmental and sequence-stratigraphic interpretation. *Earth-Sci. Rev.*, **81**, 135–174.

Dalrymple, R.W., **Zaitlin, B.A.** and **Boyd, R.** (1992) Estuarine facies models: conceptual basis and stratigraphic implications. *J. Sed. Res.*, **62**, 1130–1146.

Dalrymple, R.W., **Baker, E.K.**, **Harris, P.T.** and **Hughes, M.G.** (2003) Sedimentology and stratigraphy of a tide-dominated, foreland-basin delta (Fly River, Papua New Guinea). In: *Tropical Deltas of Southeast Asia; Sedimentology, Stratigraphy, and Petroleum Geology* (Eds F.H. Sidi, D. Nummedal, P. Imbert, H. Darman and H.W. Posamentier), *SEPM Spec. Publ.*, **76**, 147–173.

Dam, G. and **Surlyk, F.** (1993) Cyclic sedimentation in a large wave and storm-dominated anoxic lake; Kap Stewart Formation (Rhaetian-Sinemurian), Jameson Land, East Greenland. In: *Sequence Stratigraphy and Facies Associations* (Eds H.W. Posamentier, C.P. Summerhayes, B.U. Haq and G.P. Allen), *Int. Assoc. Sedimentol. Spec. Publ.*, **18**, 521–535.

Dam, G. and **Surlyk, F.** (1995) Sequence stratigraphic correlation of Lower Jurassic shallow marine and paralic successions across the Greenland-Norway seaway. In: *Sequence Stratigraphy on the Northwest European Marin* (Eds R.J. Steel, V.L. Felt, E.P. Johannessen and C. Mathieu), *Norw. Petrol. Soc. Spec. Publ.*, **5**, 483–499.

Dam, G. and **Surlyk, F.** (1998) Stratigraphy of the Neill Klinter Group; a Lower – lower Middle Jurassic tidal embayment succession, Jameson Land, East Greenland. *Geol. Greenland Surv. Bull.*, **175**, 80.

Doré, A.G. (1992) Synoptic palaeogeography of the Northeast Atlantic Seaway: Late Permian to Cretaceous. In: *Basins on the Atlantic Seaboard: Petroleum Geology, Sedimentology and Basin Evolution* (Ed. J. Parnell), *Geol. Soc. London. Spec. Publ.*, **62**, 421–446.

Dott, R.H. and **Bourgeois, J.** (1982) Hummocky stratification: significance of its variable bedding sequences. *Geol. Soc. Am. Bull.*, **93**, 663–680.

Eide, C.H., **Howell, J.A.** and **Buckley, S.J.** (2014) Distribution of discontinuous mudstone beds within shallow-marine deposits: Star Point Sandstone and Blackhawk Formation, Eastern Utah. *AAPG Bull.*, **98**, 1401–1429.

Enge, H.D., **Buckley, S.J.**, **Rotevatn, A.** and **Howell, J.A.** (2007) From outcrop to reservoir simulation model: workflow and procedures. *Geosphere*, **3**, 469–490.

Fenies, H. and **Tastet, J.-P.** (1998) Facies and architecture of an estuarine bar (the Trompeloup bar, Gironde estuary, SW France). *Mar. Geol.*, **150**, 149–169.

Filak, J.-M., **Van Lint, J.**, **Le Guerrou, E.**, **Desgoutte, N.**, **Fabre, G.**, **Ali, F.**, **Ma, E.**, **Datt, K.**, **Al-Houti, R.** and **Madhavan, S.** (2012) 3-D geological modeling of the world's largest siliciclastic reservoirs: Greater Burgan Field, Kuwait. *AAPG Search Discov. Art.*, **20169**, 32.

Gjelberg, J., **Dreyer, T.**, **Høie, A.**, **Tjelland, T.** and **Lilleng, T.** (1987) Late Triassic to Mid-Jurassic sandbody development on the Barents and mid-Norwegian shelf. In: *Petroleum Geology of North West Europe. Proceedings of the 3rd Conference* (Eds J. Brooks and K.W. Glennie), pp. 1105–1129. Graham & Trotman, London.

Hampson, G.J. (2010) Sediment dispersal and quantitative stratigraphic architecture across an ancient shelf. *Sedimentology*, **57**, 96–141.

Haq, B.U., **Hardenbol, J.** and **Vail, P.** (1987) Chronology of fluctuating sea levels since the Triassic. *Science*, **235**, 1156–1167.

Helland-Hansen, W. and **Hampson, G.J.** (2009) Trajectory analysis: concepts and applications. *Basin Res.*, **21**, 454–483.

Hori, K., **Saito, Y.**, **Zhao, Q.** and **Wang, P.** (2002) Architecture and evolution of the tide-dominated Changjian (Yangtze) River delta, China. *Sed. Geol.*, **146**, 249–264.

Hubbard, S.M., **Smith, D.G.**, **Nielsen, H.**, **Leckie, D.A.**, **Fustic, M.**, **Spencer, R.J.** and **Bloom, L.** (2011) Seismic geomorphology and sedimentology of a tidally influenced river deposit, Lower Cretaceous Athabasca oil sands, Alberta, Canada. *AAPG Bull.*, **95**, 1123–1145.

Hwang, I.-G. and **Heller, P.L.** (2002) Anatomy of a transgressive lag: Panther Tongue Sandstone, Star Point Formation, central Utah. *Sedimentology*, **49**, 977–999.

Ichaso, A.A. and **Dalrymple, R.W.** (2009) Tide- and wave generated fluid mud deposits in the Tilje Formation (Jurassic), offshore Norway. *Geology*, **37**, 539–542.

Ichaso, A.A. and **Dalrymple, R.W.** (2014) Eustatic, tectonic and climatic controls on an early syn-rift mixed-energy delta, Tilje Formation (Early Jurassic, Smørbukk Field, Offshore mid-Norway). In: *From Depositional Systems to Sedimentary Successions on the Norwegian Continental Margin* (Eds A.W. Martinius, R. Ravnås, J.A. Howell, R.J. Steel and J.P. Wonham), *Int. Assoc. Sedimentol. Spec. Publ.*, **46**, 339–388.

Kuehl, S.A., **Allison, M.A.**, **Goodbred, S.L.** and **Kudrass, H.** (2005) The Ganges-Brahmaputra Delta. In: *River Deltas: Concepts, Models, and Examples* (Eds L. Giosan and J.P. Bhattacharya), *SEPM Spec. Publ.*, **83**, 413–434.

Larsen, H.C. and **Marcussen, C.** (1992) Sill-intrusion, flood basalt emplacement and deep crustal structure of the Scoresby Sund Region, East Greenland. In: *Magmatism and the Causes of Continental Break-up* (Eds B.C. Storey, T. Alabaster and R.J. Pankhurst), *Geol. Soc. Spec. Publ.*, **68**, 365–368.

Legler, B., **Johnson, H.D.**, **Hampson, G.J.**, **Massart, B.Y.G.**, **Jackson, C.A.-L.**, **Jackson, M.D.**, **El-Barkooky, A.** and **Ravnås, R.** (2013) Facies model of a fine-grained, tide-dominated delta: Lower Dir Abu LIfa Member (Eocene), Western Desert, Egypt. *Sedimentology*, **60**, 1313–1356.

Lundin, E. and **Doré, A.G.** (2002) Mid-Cenozoic post-breakup deformation in the 'passive' margins bordering the Norwegian-Greenland Sea. *Mar. Petrol. Geol.*, **19**, 79–93.

Martinius, A.W. and **Van den Berg, J.H.** (2011) *Atlas of Sedimentary Structures in Estuarine and Tidally-Influenced River Deposits of the Rhine-Meuse-Scheldt System*. EAGE Publications BV, Houten, 298 pp.

Martinius, A.W., **Ringrose, P.S.**, **Brostrøm, C.**, **Elfenbein, C.**, **Næss, A.** and **Ringås, J.E.** (2005) Reservoir challenges of heterolithic tidal sandstone reservoir in the Halten Terrace, mid-Norway. *Petrol. Geosci.*, **11**, 3–16.

Mathiesen, A., **Bidstrup, T.** and **Christiansen, F.G.** (2000) Denudation and uplift history of the Jameson Land Basin, East Greenland – constrained from maturity and apatite fission track data. *Global Planet. Change*, **24**, 275–301.

McIlroy, D., **Flint, S.S.**, **Howell, J.A.** and **Timms, N.** (2005) Sedimentology of the tide-dominated Jurassic Lajas Formation, Neuqu en Basin, Argentina. In: *The Neuquéen Basin, Argentina: A Case Study in Sequence Stratigraphy and Basin Dynamics* (Eds G.D. Veiga, L.A. Spalletti, J.A. Howell and E. Schwarz), *Geol. Soc. London. Spec. Publ.*, **252**, 83–107.

Mjelde, R., **Breivik, A.J.**, **Raum, T.**, **Mittelstaedt, E.**, **Ito, G.** and **Faleide, J.I.** (2008) Magmatic and tectonic evolution of the North Atlantic. *J. Geol. Soc. London*, **165**, 31–42.

Nystuen, J.P., **Kjemperud, A.V.**, **Müller, R.**, **Adestål, V.** and **Schomacker, E.R.** (2014) Late Triassic to Early Jurassic climatic change, northern North Sea region: impact on alluvial architecture, palaeosols and clay mineralogy. In: *From Depositional Systems to Sedimentary Successions on the Norwegian Continental Shelf* (Eds A.W. Martinius, R. Ravnås, J.A. Howell, R.J. Steel and J.P. Wonham), *Int. Assoc. Sedimentol. Spec. Publ.*, **46**, 291–333.

Olariu, M., **Olariu, C.**, **Steel, R.J.**, **Dalrymple, R.W.** and **Martinius, A.W.** (2012) Anatomy of a laterally migrating tidal bar in front of a delta system: Esdolomada Member, Roda Formation, Tremp-Graus Basin, Spain. *Sedimentology*, **59**, 356–378.

Plint, A.G. (1996) Marine and nonmarine systems tracts in fourth-order sequences in the Early-Middle Cenomanian, Dunvegan Alloformation, northeastern British Columbia, Canada. *Geol. Soc. London. Spec. Publ.*, **104**, 159–191.

Pontén, A. and **Plink-björklund, P.** (2007) Depositional environments in an extensive tide-influenced delta plain, Middle Devonian Gauja Formation, Devonian Baltic Basin. *Sedimentology*, **54**, 969–1006.

Pontén, A. and **Plink-Björklund, P.** (2009) Regressive to transgressive transits reflected in tidal bars, Middle Devonian Baltic Basin. *Sed. Geol.*, **218**, 48–60.

Rittersbacher, A., **Buckley, S.J.**, **Howell, J.A.**, **Hampson, G.J.** and **Vallet, J.** (2014) Helicopter-based laser scanning: a method for quantitative analysis of large-scale sedimentary architecture, *Geol. Soc. London. Spec. Publ.*, **387**, 185–202.

Slama, J., **Walderhaug, O.**, **Fonneland, H.**, **Kosler, J.** and **Pedersen, R.B.** (2011) Provenance of Neoproterozoic to upper Cretaceous sedimentary rocks, eastern Greenland: implications for recognizing the sources of sediments in the Norwegian Sea. *Sed. Geol.*, **238**, 254–267.

Smith, A.G., **Smith, D.G.** and **Funnell, B.M.** (1994) *Atlas of Mesozoic and Cenozoic Coastlines*. Cambridge University Press, Cambridge, UK, 99 pp.

Storms, J.E.A., **Hoogendoorn, R.M.**, **Dam, A.C.R.**, **Hoitink, A.J.F.** and **Kroonenberg, S.B.** (2005) Late-Holocene evolution of the Mahakam delta, East Kalimantan, Indonesia. *Sed. Geol.*, **180**, 149–166.

Surlyk, F. (2003) The Jurassic of East Greenland: a sedimentary record of thermal subsidence, onset and culmination of rifting. In: *The Jurassic of Denmark and*

Greenland (Eds J.R. Ineson and F. Surlyk), *Geol. Surv. Denmark Greenland Bull.*, **1**, 659–722.

Surlyk, F., **Callomon, J.H.**, **Bromley, R.G.** and **Birkelund, T.** (1973) *Stratigraphy of the Jurassic-Lower Cretaceous sediments of Jameson Land and Scoresby Land, East Greenland* Bianco Lunas Bogtrykkeri. , Copenhagen.

Täanavsuu-Milkeviciene, K. and **Plink-Björklund, P.** (2009) Recognizing tide-dominated versus tide-influenced deltas: Middle Devonian strata of the Baltic Basin. *J. Sed. Res.*, **79**, 887–905.

Taylor, A.M. and **Goldring, R.** (1993) Description and analysis of bioturbation and ichnofabric. *J. Geol. Soc. London*, **150**, 141–148.

Thomas, R.G., **Smith, D.G.**, **Wood, J.M.**, **Visser, J.**, **Calverley-Range, E.A.** and **Koster, E.H.** (1987) Inclined Heterolithic Stratification – terminology, description and significance. *Sed. Geol.*, **53**, 123–179.

Vakarelov, B.K. and **Ainsworth, R.B.** (2013) A hierarchical approach to architectural classification in marginal-marine systems: bridging the gap between sedimentology and sequence stratigraphy. *AAPG Bull.*, **97**, 1121–1161.

Vallet, J. and **Skaloud, J.** (2004) Development and experiences with a fully-digital handheld mapping system operated from a helicopter. *Int. Arch. Photogrammetry Remote Sens. Spatial Inform. Sci.*, **35** (Part B5), 1–6.

Van den Berg, J.H., **Boersma, J.R.** and **Van Gelder, A.** (2007) Diagnostic sedimentary structures of the fluvial-tidal transition zone – evidence from deposits of the Rhine and Meuse. *Neth. J. Geosci.*, **86**, 287–306.

Van Wagoner, J.C., **Mitchum, R.M.**, **Campion, K.M.** and **Rahmanian, V.D.** (1990) Siliciclastic sequence stratigraphy in well logs, cores and outcrops. *AAPG Meth. Explor. Ser.*, **7**, 55.

Visser, M.J. (1980) Neap-spring cycles reflected in Holocene subtiral large-scale bedform deposits: a preliminary note. *Geology*, **8**, 543–546.

Willis, B.J. (2005) Deposits of tide-influenced river deltas. In: *River Deltas; Concepts, Models, and Examples* (Eds L. Giosan and J.P. Bhattacharya), *SEPM Spec. Publ.*, **83**, 87–129.

Willis, B.J. and **Gabel, S.** (2001) Sharp-based tide-dominated deltas of the Sego Sandstone, Book Cliffs, Utah, USA. *Sedimentology*, **48**, 479–506.

Willis, B.J. and **Gabel, S.** (2003) Formation of deep incisions into tide-dominated river deltas: implications for the stratigraphy of the Sego Sandstone, Book Cliffs, Utah, USA. *J. Sed. Res.*, **73**, 246–263.

Willis, B.J., **Bhattacharya, J.P.**, **Gabel, S.L.** and **White, C.D.** (1999) Architecture of a tide-influenced river delta in the Frontier Formation of central Wyoming, USA. *Sedimentology*, **46**, 667–688.

Ziegler, P. (1988) Evolution of the Arctic – North Atlantic and the western Tethys. *AAPG Mem.*, **43**, 198.

Manuscript received 19 February 2015; revision accepted 27 January 2016